

**Dissertation**

**Master of Science**

**Vanessa Rheinheimer**

**2008**

ADVANCED MASTERS IN STRUCTURAL ANALYSIS OF MONUMENTS AND HISTORICAL  
CONSTRUCTIONS

CZECH TECHNICAL UNIVERSITY IN PRAGUE, CZECH REPUBLIC  
TECHNICAL UNIVERSITY OF CATALONIA, SPAIN

## **SULPHATE ATTACK AND THE ROLE OF THAUMASITE IN HISTORICAL CONSTRUCTIONS**

Dissertation submitted to Czech Technical University in Prague and Technical University of Catalonia as a partial requisite to obtain the title of Master of Science for the Advanced Masters in Structural Analysis of Monuments and Historical Constructions.

**Vanessa Rheinheimer**

Barcelona, Spain, July 2008.

*“While going down a slope, Zorba kicked against a stone, which went rolling downhill. He stopped for a moment in amazement, as if he were seeing this astounding spectacle for the first time in his life. He looked round at me, and in his look I discerned faint consternation.*

*‘Boss, did you see that?’ he said at last. ‘On slopes, stones come to life again’.*

*I said nothing, but I felt a deep joy. This, I thought, is how great visionaries and poets see everything – as if for the first time. Each morning they see a new world before their eyes; they do not really see it, they create it.*

*The universe for Zorba, as for the first men on earth, was a weighty, intense vision; the stars glided over him, the sea broke against his temples. He lived the earth, the water, the animals and God, without the distorting intervention of reason.”*

*(Nikos Kazantzakis in Zorba, the Greek)*

*To my father, who makes it possible,  
and my sisters, whom make me strong.*

## ACKNOWLEDGMENT

I would like to thank my advisor, Professor Lucia Fernandez Carrasco, for the guidance, patience and friendship during this time. Besides I would like to thanks the Materials section and Department of Construction Engineering of UPC, and also for the Instituto de Ciencias de la Construcción Eduardo Torroja for the collaboration to the development of this research.

I also want to thank the SAHC coordination, for the great opportunity of participate of this course, and to all the professors of the course for the knowledge, the guidance and friendship. For the Erasmus Mundus Program, for the scholarship that allowed me to join this course.

I particularly want to thank Professor Ignasi Casanova, for believing in my potential and helping me for a long time.

My father, my main teacher, for giving me opportunity to realize my dreams and believe that I can realize it. And my sisters, for all the incentive and support. The distance made it difficult, but your sweet words always made me believe it is possible. Thanks Gisa also, for taking care of my family.

To all my friends, in special to Ana Paula: distance is nothing for us! (You made it possible) And for my great friend-sister Bilge, for all the time we spent together: study, trips, books, football and music, soups, English and Portuguese classes... thanks for everything! Thanks also to all my friends in Brazil for help me online and never lose the contact: Markinho, Raphael, Arthur, Camila, Van, Pri, Aline, and Tati. And here, new and old friends: Shweta, Hui Yin, Roberto, Juan, Luis and Anibal, Daniel, Gloria, Felipe, Aninha and Ângela, for support, help and teach me. Also to all my course colleagues.

Thanks for CVUT for the reception, in special to Professor Petr Kabele and to our tutor Natalia Cavina, for all the help during the time in Prague. And to UPC, especially to Professor Pere Roca, for the PhD students Elaine, Ana, Mauro, Desilvia, Diego, for receive me as a family, and for Mati and Eufronio for all the help and advice at the laboratory.

## ABSTRACT

*Rheinheimer, Vanessa. Sulphate Attack and the Role of Thaumasite in Historical Constructions. 2008. Dissertation (Master of Science). Advanced Masters in Structural Analysis of Monuments and Historical Constructions. Czech Technical University in Prague and Technical University of Catalonia. Barcelona. Spain.*

Some of important historic constructions around the world are located in centers of big cities, many times near to industrial areas and regarding of that it can be submitted to sulphate atmosphere, important degradation factor for the durability and serviceability of cementitious systems. On the other hand, in the architectural and monumental heritage, it is possible to find masonry with different types of mortars, or also with ancient concrete, cementitious materials subject to suffer sulphate attack. The attack on the cementitious system may occur in different ways: delayed ettringite formation, gypsum formation or, when there is a source of carbonate, thaumasite formation, object of this study. The thaumasite was found in 1965 in decayed concrete and in repairing mortars used for the conservation of the architectural heritage, and its formation is generally associated with relatively cold climate conditions, but nowadays the formation process of thaumasite is still not been explained. Thaumasite can be formed through a combination of sulphate attack and carbonation, and occur in concrete structures and in masonry walls of historic buildings. It provokes expansion, cracking, spalling, loss of strength and adhesion of cementitious materials, transforming hardened concretes or mortars in a pulpy mass because of the loss of strength. Regarding to the identification of the composite, the crystallographic structure of ettringite and thaumasite is very similar, in spite of the difference between their chemical composition, and consequently, the X-Ray diffraction patterns for this two composites are very similar. For this reason, different techniques are used together to identify and differentiate this composites. To develop this research, pastes were prepared and carbonated in laboratory under carbonation and sulphate conditions. The evolution of the mineralogy of the pastes was monitored through time with the aid of X-Ray Diffraction and Fourier Transform Infra-Red. In parallel, compressive and tensile strength were measured. The data sets were analysed to find interrelationships regarding to understand the effect of CO<sub>2</sub>, temperature and time in the formation of as ettringite and thaumasite. The results shows the sulphate attack products formation with the increasing of ettringite, but not the thaumasite formation after this exposition period.

*Keywords: Sulphate attack; Thaumasite; Historical constructions.*

## RESUMEN

*Rheinheimer, Vanessa. Ataque por sulfatos y el papel de la Taumasita en construcciones históricas. 2008. Tesis (Master of Science). Advanced Masters in Structural Analysis of Monuments and Historical Constructions. Czech Technical University in Prague and Technical University of Catalonia. Barcelona. Spain.*

Gran parte de construcciones históricas importantes se encuentran en el centro de grandes ciudades, y en ocasiones próximas a la industria y por ello en contacto con áreas que presentan una atmósfera rica en sulfatos, siendo este factor de considerable importancia sobre la durabilidad y procesos de degradación y por tanto en las prestaciones de los sistemas de cemento. Por otra parte, en la arquitectura y el patrimonio monumental es posible encontrar mampostería con diferentes tipos de morteros o también con antiguos hormigones y materiales cementantes que pueden ser susceptibles de sufrir ataque sulfático. Tal ataque por sulfatos puede producirse de diferentes maneras: formación de etringita retrasada, formación del yeso, o formación de taumasita cuando hay una fuente de carbonatos, objetivo de este estudio. La taumasita se encontró en 1965 en hormigón degradado y en la reparación de morteros utilizados para la conservación del patrimonio arquitectónico; y aunque su formación se asocia generalmente con clima relativamente frío, en la actualidad el proceso de formación de taumasita aún no se ha explicado. La taumasita puede formarse mediante la combinación de ataque por sulfatos y carbonatación y se ha detectado en estructuras de hormigón y también en albañilería en paredes de edificios históricos. La formación de taumasita puede provocar expansión, agrietamiento, desagregación, pérdida de adherencia de los materiales de cemento, transformar hormigones endurecidos o morteros en una masa pulverulenta debido a la pérdida de resistencia. En lo que respecta a la identificación de los compuestos, la estructura cristalográfica de la etringita y la taumasita es muy similar, a pesar de la diferencia entre su composición química y, en consecuencia, los patrones de difracción de Rayos-X de estos dos compuestos son muy similares. Por esta razón, diferentes técnicas se utilizan juntas para identificar y diferenciar este compuestos. Para desarrollar esta investigación, se prepararon probetas de pasta que fueron caracterizadas tanto mineralógicamente como mecánicamente y posteriormente fueron carbonatadas en el laboratorio y sometidas a la acción de los sulfatos. La evolución mineralógica de las pastas se ha analizado mediante difracción de rayos-X y espectroscopia de infrarrojo por transformada de Fourier. Se ha analizado la influencia del cemento, de la presencia de humo de sílice así como del tipo y del tiempo de carbonatación sobre en la formación de de productos debidos a ataque sulfatito y formación de taumasita. Los resultados muestran los productos formados por el ataque por sulfatos con el aumento de la etringita, pero no hay formación de taumasita no período disponible para la realización de la recerca.

*Palabras clave: Ataque sulfatico, taumasita, construcciones históricas.*

## RESUMO

*Rheinheimer, Vanessa. Ataque por Sulfatos e o papel da Thaumasita em Edificações Históricas. 2008. Dissertação (Master of Science). Advanced Masters in Structural Analysis of Monuments and Historical Constructions. Czech Technical University in Prague and Technical University of Catalonia. Barcelona. Espanha..*

Algumas das importantes edificações históricas no mundo se localizam em centros de grandes cidades, muitas vezes perto de zonas industriais, o que pode submetê-las a um ambiente com sulfatos, importante fator de degradação para a durabilidade e vida útil de sistemas cimentícios. Por outro lado, em patrimônios arquitetônicos e monumentos é possível encontrar materiais suscetíveis a sofrer ataque por sulfatos, o qual pode ocorrer de diferentes maneiras: através de formação de etringita secundária, formação de gipsita ou ainda, quando há uma fonte de carbonatos, formação de taumasita, objeto deste estudo. A taumasita foi encontrada em 1965 em concretos deteriorados e argamassas para reparo usadas na conservação de patrimônio arquitetônico, e sua formação está normalmente associada a climas frios. Contudo, o processo de formação deste composto ainda não é perfeitamente conhecido. A taumasita pode ser formada por uma combinação de ataque por sulfatos e carbonatação, e pode ocorrer em estruturas de concreto e paredes de alvenaria em edifícios históricos. Isto provoca expansão, fissuras, lascas, perda de resistência e coesão dos materiais cimentícios, transformando o concreto endurecido ou argamassas em uma massa pulverulenta pela perda de resistência. Quanto à identificação deste composto, a estrutura cristalográfica da etringita e da taumasita é muito similar, apesar de sua diferença na composição química e, conseqüentemente, a difração de Raios-X para estes dois compostos é muito similar. Por este motivo, diferentes técnicas são utilizadas em conjunto para facilitar a identificação e diferenciação destes compostos. Para o desenvolvimento desta pesquisa, pastas foram preparadas e carbonatadas em laboratório em condições de carbono e sulfatos. A evolução da mineralogia das pastas durante o tempo foi monitorada através de ensaios de Difração de raios-X e Transformada de Fourier para Infra-vermelho. Paralelamente, resistências à compressão e tração na flexão foram medidas. Os resultados foram analisados visando encontrar relações que permitam entender o efeito do Gás Carbônico, temperatura e tempo na formação de etringita e taumasita. Os resultados mostram os produtos resultantes do ataque por sulfatos com a formação de etringita, porém não ocorre a formação de taumasita no tempo disponível para a reação desta pesquisa.

*Palavras-chave: Taumasita; Ataque por sulfatos; Edificações históricas.*



## CONTENTS

FIGURE LIST	xi
TABLE LIST	xiv
Cement chemical nomenclature	xv
<b>1 INTRODUCTION</b>	<b>1</b>
1.1 Dissertation Objectives	2
1.1.1 General Objectives	2
1.1.2 Specific Objectives	2
1.2 Outline of the Dissertation	3
<b>2 PORTLAND CEMENT</b>	<b>4</b>
2.1 Composition of Cement Phases	9
2.1.1 Alite	9
2.1.2 Belite	10
2.1.3 Calcium Aluminate	11
2.1.4 Ferrite	12
2.1.5 Minor constituents	13
2.2 Types of Cements	13
2.3 Hydration mechanisms	15
2.4 Hydration products	18
2.5 Influence of Silica Fume addition	19
<b>3 DURABILITY</b>	<b>20</b>
3.1 Carbonation	21
3.2 Sulphate Attack	22
3.2.1 Mechanism of attack	25
3.3 Thaumasite	27
3.3.1 Formation conditions	33
3.3.2 Identification	36
3.3.3 Historical cases	38
<b>4 MATERIALS AND METHODS</b>	<b>43</b>
4.1 Materials	43
4.1.1 Cement	43
4.1.2 Silica Fume	46
4.2 Methodology	47
4.2.1 Experimental set up	48
4.3 Analytical methods	50
4.3.1 X-Ray fluorescence	51
4.3.2 Fourier Transform Infra-Red – FTIR	52
<b>5 RESULTS AND ANALYSIS</b>	<b>54</b>
5.1 Binder systems before carbonation exposure	54
5.1.1 Influence of type of cement	54

5.1.2	Mechanical Tests	56
5.2	Binder systems after carbonation exposure	58
5.2.1	Influence of carbonation system	63
5.3	Binder systems after sulphate exposure	63
6	FINAL CONSIDERATIONS	68
6.1	Conclusions	68
6.2	Suggestions for future researches	70
	BIBLIOGRAPHY	71

## FIGURE LIST

- Figure 1 Hadrian's Wall, England, a few miles east of Housesteads was built in A.D. 122 by three Roman Legions, using local materials available, and in some parts the stone faced an inner core composed of concrete and rubble (Source: [www.understandin-cement.com](http://www.understandin-cement.com)). \_\_\_\_\_ 5
- Figure 2 Graph of hydration stages and schematic representation of anhydrous cement particle. At the graph, I represents the beginning of the heat evolution regarding to the partial dissolution of the cement and beginning of C3A and C3S hydration. II represents the induction or sleeping period, with low heat release, indicating the C3A hydration control. III shows the retaking of the reactions and increasing of heat. IV represents the reduction in the quantity of sulphate ions. In the drawings, (a) shows the anhydrous cement particle, (b) presents the effect after around 10 minutes, (c) after 10 hours, (d) after 18 hours, (e) after 1-3 days and (f) after 2 weeks. (Kirchheim, 2008 - compilation from Scrivener, 1984 and Bishop, 2003). \_\_\_\_\_ 16
- Figure 3 Cement hydration (Source: M. G. Juenger, P. J. M. Monteiro, E. Gartner. UC Berkeley, and G. Denbeaux, LBNL). \_\_\_\_\_ 18
- Figure 4 Crystal structure of thaumasite—projection on a – b plane (Torres et al, 2004). \_\_\_\_\_ 29
- Figure 5 Polished section of degraded concrete from a highways structure in the United Kingdom. Thaumasite has formed around coarse limestone aggregate (large dark particles) and in cracks. Examples of thaumasite are arrowed. This polished section was 40mm in diameter but thaumasite formation is so extensive that it requires little magnification to be clearly visible (Source: [www.understandin-cement.com](http://www.understandin-cement.com)). \_\_\_\_\_ 30
- Figure 6 Sketch of the idealized form taken by TSA degradation with high quality structural concrete (Sibbick and Crammond, 2003). \_\_\_\_\_ 32
- Figure 7 The phase composition of a blended cement with 15 wt.% raw feed precipitator dust shown as a function of the CaSO<sub>4</sub> content. Thaumasite is assumed to be a stable phase (Juel et al., 2003). \_\_\_\_\_ 35
- Figure 8 Projection of the relevant phases on to sub-ternary compatibility diagram for the C3A–CaCO<sub>3</sub>–CaSO<sub>4</sub> system showing the relative contents of the phases (Juel et al., 2003). \_\_\_\_\_ 36
- Figure 9 Thaumasite and Ettringite XRD patterns (Collepari, 1999). \_\_\_\_\_ 37
- Figure 10 (a) Thaumasite efflorescence on the internal side of a brick wall exposed to north. (b) External brick wall exposed to south without thaumasite efflorescence (Veniale et al, 2003). \_\_\_\_\_ 39
- Figure 11 Deterioration of the rendering mortar caused by ettringite (a) and thaumasite (b) formation in a building located in the historical centre of Ancona (Corinaldesi et al, 2003). \_\_\_\_\_ 40
- Figure 12 Bridge in Amsterdam. (a) View. (b) Damage to masonry in vault intrados (van Hees et al, 2003). \_\_\_\_\_ 41

Figure 13 Church tower in Noordwijk, with both vertical and horizontal cracks (van Hees et al, 2003). _____	42
Figure 14 X-Ray Diffraction for the anhydrous cements. _____	44
Figure 15 Fourier Transform Infra-Red for the cements. _____	44
Figure 16 Laser granulometry of the cements. _____	45
Figure 17 Fourier Transform Infra-Red for the silica fume. _____	46
Figure 18 X-Ray Diffraction for the silica fume. _____	46
Figure 19 Laser granulometry of the silica fume. _____	47
Figure 20 Samples. _____	49
Figure 21 Samples at carbonation chambers. _____	50
Figure 22 Ages of the tests. _____	50
Figure 23 Samples grounding. _____	51
Figure 24 Stopping the hydration of the Samples. _____	51
Figure 25 X-Ray diffraction results of Portland cement systems before start the carbonation. _____	55
Figure 26 FTIR results of Portland cement systems before start the carbonation. _____	55
Figure 27 Compression Resistance of the mortars. _____	56
Figure 28 Flexure Resistance of the mortars. _____	57
Figure 29 X-Ray diffraction results of Portland cement systems after 15 days of CO <sub>2</sub> exposition. _____	58
Figure 30 FTIR results of Portland cement systems after 15 days of CO <sub>2</sub> exposition. _____	58
Figure 31 X-Ray diffraction results of Portland cement systems after 30 days of CO <sub>2</sub> exposition. _____	59
Figure 32 FTIR results of Portland cement systems after 30 days of CO <sub>2</sub> exposition. _____	59
Figure 33 X-Ray diffraction results of Portland cement systems after 15 days of air exposition. _____	60
Figure 34 FTIR results of Portland cement systems after 15 days of air exposition. _____	61
Figure 35 X-Ray diffraction results of Portland cement systems after 30 days of air exposition. _____	61
Figure 36 FTIR results of Portland cement systems after 30 days of air exposition. _____	62
Figure 37 X-Ray diffraction results of Portland cement systems after 15 days of CO <sub>2</sub> exposition and 30 days of sulphate exposition. _____	63
Figure 38 FTIR results of Portland cement systems after 15 days of CO <sub>2</sub> exposition and 30 days of sulphate exposition. _____	64
Figure 39 X-Ray diffraction results of Portland cement systems after 15 days of air exposition and 30 days of sulphate exposition. _____	64
Figure 40 FTIR results of Portland cement systems after 15 days of air exposition and 30 days of sulphate exposition. _____	65

Figure 41 X-Ray diffraction results of Portland cement systems after 30 days of CO <sub>2</sub> exposition and 30 days of sulphate exposition. _____	65
Figure 42 FTIR results of Portland cement systems after 30 days of CO <sub>2</sub> exposition and 30 days of sulphate exposition. _____	66
Figure 43 X-Ray diffraction results of Portland cement systems after 30 days of air exposition and 30 days of sulphate exposition. _____	66
Figure 44 FTIR results of Portland cement systems after 30 days of air exposition and 30 days of sulphate exposition. _____	67

**TABLE LIST**

Table 1 Types of cements according to UNE-EN 197:2000. _____	13
Table 2 Types and subtypes of cement according to UNE-EN 197:2000. _____	14
Table 3 Types of additions according to UNE-EN 197:2000. _____	14
Table 4 Sulphate resistant cements according to UNE 80303:2001. _____	15
Table 5 Chemical analysis of the cements. _____	43
Table 6 Granulometric distribution of the cements. _____	45
Table 7 Granulometric distribution of the silica fume. _____	47
Table 8 Initial and final setting time. _____	48
Table 9 Infrared Spectral Data for the Calcium Aluminate Sulphate Hydrates (Source: Bensted, J. An Infrared Spectral Examination of Calcium Aluminate Hydrates and Calcium Aluminate Sulphate Hydrates encountered in Portland cement Hydration). _____	53
Table 10 Compression Strength of the mortars. _____	56
Table 11 Flexure Resistance of the mortars. _____	57

### Cement chemical nomenclature

Name	Composition	Nomenclature
Lime	CaO	C
Silica	SiO <sub>2</sub>	S
Alumina	Al <sub>2</sub> O <sub>3</sub>	A
Iron	Fe <sub>2</sub> O <sub>3</sub>	F
Water	H <sub>2</sub> O	H
Sulfuric anhydride	SO <sub>3</sub>	S
Magnesia	MgO	M
Soda	Na <sub>2</sub> O	N
Potassa	K <sub>2</sub> O	K
Tricalcium Silicate (Alite)	$3CaO \cdot SiO_2$	C <sub>3</sub> S
β-Dicalcium Silicate (Belite)	$2CaO \cdot SiO_2$	C <sub>2</sub> S
Tricalcium Aluminate	$3CaO \cdot Al_2O_3$	C <sub>3</sub> A
Calcium Silicate Hydrated	$3CaO \cdot 2SiO_2 \cdot 3H_2O$	C-S-H
Calcium hydroxide (Portlandite)	$Ca(OH)_2$	CH

## 1 INTRODUCTION

Majority of historic constructions around the world are located in centers of big cities, most of the times near to industrial areas, and as a result of this fact they are subjected to atmosphere with high sulphate content which is important degradation factor for the durability and serviceability of cementitious systems.

On the other hand, in cultural heritage buildings that encompass thousands of years, a variety of mortars has been used including early concrete and cementitious mortars that might be vulnerable to sulphate attack.

The sulphate attack at cementitious systems may occur in different ways: delayed ettringite formation, gypsum formation or, when there is a source of carbonate, thaumasite formation.

The thaumasite was found in 1965 in decayed concrete and in repairing mortars used for the conservation of the architectural heritage, and its formation is generally associated with relatively cold climate conditions, but nowadays the formation process of thaumasite is still not clearly explained.

Thaumasite can be formed through a combination of sulphate attack and carbonation, and occurs at concrete structures and at masonry walls of historic buildings. It provokes expansion, cracking, spalling, loss of strength and adhesion of cementitious materials, transforming hardened concretes or mortars in a pulpy mass due to loss of strength.

Regarding the identification of the composite, the crystallographic structure of ettringite and thaumasite is very similar, in spite of the difference between their chemical composition, and consequently, the X-Ray diffraction patterns for this two composites is very alike. For this reason, different techniques are used together to identify and differentiate this composites.

Moreover it is known that sulphate resistant cement do not prevent the thaumasite formation, but the addition of some types of pozzolan such as silica fume promote the decreasing on porosity and improve the resistance to the entrance of the aggressive agent.



The aim of the present research concerns with the study of the effect of carbonation type and time in specimens of pastes with different rate of gel C-S-H; moreover the effect over sulphate resistant cement is also evaluated.

## ***1.1 Dissertation Objectives***

The main focus of this dissertation is to investigate the influence of the external carbonate acting on the formation of thaumasite under external sulphate attack.

### **1.1.1 General Objectives**

The main focus of this dissertation is to investigate the thaumasite formation in samples submitted to carbonation and external sulphate attack process.

This project aims at putting additional constraints on thaumasite formation and apply the results to several case studies where sulphate attack is known to have played a prominent role in the deterioration of historical constructions.

### **1.1.2 Specific Objectives**

The deliverables expected from this study are:

- Describe the thaumasite formation process in cementitious materials in the context of durability, considering thaumasite formation and thaumasite for sulphate attack;
- Present cases of thaumasite degradation in historical constructions;
- Evaluate the sulphate attack progress and thaumasite formation in samples submitted to carbonation and sulphates.

## ***1.2 Outline of the Dissertation***

The dissertation is composed of six chapters, according to the description followed:

Chapter two gives an overview on Portland cement history, its composition, hydration process and its different types and classification according to the Spanish Standards.

Chapter three presents aspects related to the durability of cementitious systems, focusing in carbonation, sulphate attack and thaumasite formation, summarizing the key points of this study.

Chapter four presents the experimental program developed in this research, describing the materials, techniques and tests performed to investigate the thaumasite formation.

Chapter five gives the results of the tests performed during this research, and the analysis of this results.

Chapter six concludes this dissertation with a summary of the results obtained for the thaumasite formation, as well presents suggestions for future researches.

## 2 PORTLAND CEMENT

In ancient constructions, materials used as mortar components were chosen according to the availability in the region, since transport was very expensive or unpractical. Regarding this factor, materials from different origins have been used to produce mortar around the world (Balén et al, 1999).

Historically, the techniques of producing hydraulic mortars was dominated around the 10<sup>th</sup> century BC by the Phoenicians and the Israelites, generally obtained by mixing lime and crushed ceramics (cocciopesto). After that, pozzolanic<sup>1</sup> sand was used by Greeks, and a type of sand of volcanic origin, present near Pozzouli (which give the name pozzolanic), was used by Romans in a concrete-like masonry made of crushed stone pieces with burned lime and water as binding material with a good performance to produce hydraulic mortars. This was principally due to the presence of silica (SiO<sub>2</sub>) and alumina (Al<sub>2</sub>O<sub>3</sub>), both amorphous, that have a vitreous state and high specific surface area; those characteristics allow it to react with lime and water to form calcium silicates and aluminates hydrates (Balén et al, 1999; Popovics, 1992). An example of Roman construction using ancient cement is presented in Figure 1.

---

<sup>1</sup> Pozzolan is a vitreous siliceous or aluminosiliceous material used to produce hydraulic cement. In the beginning just as volcanic ash, but nowadays the most used pozzolans are fly ash, silica fume, high reactivity metakaolin, ground granulated blast furnace slag, among others. Modern pozzolanic cements are a mix of natural or industrial pozzolans and Portland cement.



**Figure 1 Hadrian's Wall, England, a few miles east of Housesteads was built in A.D. 122 by three Roman Legions, using local materials available, and in some parts the stone faced an inner core composed of concrete and rubble (Source: [www.understandin-cement.com](http://www.understandin-cement.com)).**

After that, just in 16<sup>th</sup> century the Italian architect Andrea Palladio identified the hydraulic lime, which can harden under water without pozzolans. Later, in 1756, Smeaton discovered the hydraulic reactions which occur in the process of formation of hydraulic lime, which was called Roman Cement at that time.

Independently, Vicat and J. F. John found that 25 to 30% of clay addition to limestone produces the best hydraulic lime. Vicat's research produced a cement which can be placed between lime hydrate and the actual Portland cement (Balén et al, 1999; Popovics, 1992).

In 1824 the British Joseph Aspdin took out a patent for a denominated "cement of superior quality" resembling Portland stone, which was called Portland cement, but this material was probably hydraulic lime because of the apparently low burning temperature used. Just 20 years later, Isaac C. Johnson started the production of Portland cement in the modern sense, but just in 1868 W. Michaelis provided further development on the technology analyzing the most favorable composition of the raw materials for Portland cement (Popovics, 1992).

After that, during the years different materials were used looking forward different behaviors for the concrete to be used in several conditions, and in 1919 F. Ferrari produced in Italy the first Portland cement with improved sulphate resistance (Popovics, 1992).

Nowadays the Portland cement is the most used type of cement. It is formed by heating materials from geologic origin, usually limestone and around 20 to 30% of clay

content, or other materials of similar bulk composition and sufficient reactivity until the partial fusion, which occurs at approximately 1450°C. This process forms the clinker<sup>2</sup>, it is cooled and milled to a specific surface area around 3000 to 5000 cm<sup>2</sup>/gr, and finely ground with around 3 to 5% of a setting regulator, which is generally gypsum, to make the cement (Balen et al, 1999; Taylor, 1990).

The gypsum is added to control the rate of set and may be partly replaced by other forms of calcium sulphate. The composition of clinker is typically around 67% of CaO, 22% of SiO<sub>2</sub>, 5% of Al<sub>2</sub>O<sub>3</sub>, 3% of Fe<sub>2</sub>O<sub>3</sub> and 3% of other components (Taylor, 1990).

According to Ramachandran et al (2002) the sequence of reactions which occurs during the clinker production is as follows:

- Temperature around 100°C (drying zone): free water is expelled;
- Pre-heating zone (100–750°C): firmly bound water from the clay is lost;
- Calcining zone (750–1000°C): calcium carbonate is dissociated eliminating CO<sub>2</sub>;
- Burning zone (1000–1450°C): partial fusion of the mix occurs, with the formation of C<sub>3</sub>S, C<sub>2</sub>S;
- Cooling zone (1450–1300°C), crystallization occurs with the formation of calcium aluminate and calcium aluminoferrite in form of clinker.

At architectural and monumental heritage is possible to find masonry with different kinds of mortars, according to Balen et al (1999), such as:

- in masonry dating up to the mid-19th century:
  - original air-hardening mortars, as gypsum and lime mortars;
  - original hydraulic mortars, as pozzolans and hydraulic lime mortars;
  - restoration mortars, such as gypsum, lime and hydraulic mortars.
- in masonry dating from the mid-19th century onwards:

---

<sup>2</sup> Clinker is the solid material produced by the cement kiln stage that has sintered into lumps or nodules.

- original hydraulic mortars, as hydraulic lime and cement mortars;
- restoration mortars, as hydraulic mortars and organic additive mortars.

Resuming, most of mortars find in constructions of the Historical Heritage are be constituted by lime binders or lime with pozzolana or portland cement. Based on this fact, Palomo et al details this kinds of historical mortars:

Firstly, mortars based on lime use as a binder calcium hydroxide, which produces  $\text{CaCO}_3$  when carbonated, responsible for the hardening of the material. Its main constituents are calcium oxide and calcium hydroxide ( $\text{CaO}$ ,  $\text{Ca(OH)}_2$ ), magnesium oxide and hydroxide ( $\text{MgO}$ ,  $\text{Mg(OH)}_2$ ), silica ( $\text{SiO}_2$ ), alumina ( $\text{Al}_2\text{O}_3$ ) and iron oxide ( $\text{Fe}_2\text{O}_3$ ).

The lime mortars present low mechanical strengths, due to the low affinity of the calcite and quartz crystal, as well as to the weak linkage among the calcite particles. It has an easy workability, due to the slow process of setting (carbonation) that depends on the environmental conditions and high capacity of deformation (low module of elasticity). It allows the material to absorb small movements of the adjacent materials. On the other hand, it presents an high permeability to water and water vapour, but low resistance to freeze-thaw cycles.

The limes used in this mortars can be:

- Air lime, constituted by calcium oxide (unslaked lime) and/or hydroxide (slaked lime). In this case, the addition of water is for to facilitate the mixture of the components and placing the mortar, but it does not intervene in any chemical reaction. The hardening of the mortar takes place for the reaction of the  $\text{Ca(OH)}_2$  with the atmospheric  $\text{CO}_2$  producing  $\text{CaCO}_3$ . This product provides the mortar physical, chemical and mechanical properties.
- Hydraulic lime, predominantly calcium silicates, calcium aluminates and calcium hydroxide. The addition of water intervenes in chemical reactions with silicates and aluminates (both present in the raw materials) generating the formation of hydrated compounds that confer the mortar some different properties to those obtained in the case of the air limes.

This kind of mortars do not have presence of soluble salts which avoid the processes of dissolution-crystallization of the salts, and therefore result in the appearance of efflorescence and subflorescences.

Secondly, Palomo et al describe the mortars based on portland cement binders which, when mixed with water, form a slug that harden and gives stable products with time. In the presence of water, the silicates and aluminates present in cement form products of hydration which in time produce the hydrated cement paste as a stiff and hard mass. These products of hydration have very low solubility in water. This process will be described in details in Item 2.3.

The hydrated portland cement have stability of volume, due to the fact that with the hydration process a mortar undergoes shrinkage due to a volume decrease of the hydrated cement phases. Additionally, the so called hydraulic retraction is also produced; it occurs because of the quick evaporation of the water of the plastic mass. In addition, it is resistant to the chemical aggression, if the mortar has been carefully elaborated (well compacted, no cracks, low porosity, appropriate binder/water ratio, etc.), providing good durability. Moreover, it has high mechanical strengths due to the formation of a high proportion of C-S-H gel. On the other hand, the hydration reactions of Portland cement phases are exothermal. The fast development of heat in the system can lead to a quick evaporation of water which could results to the formation of cracks in the mortar.

Finally, the authors describe other mortars, which can be find in historical constructions, based on lime and pozzolanic materials, that are natural substances or industrial by-products having an amorphous or partially crystalline structure formed by silica, silico-aluminium compounds or a combination of both composition. This materials do not harden when mixed with water, but when powdered, they are able to react with the calcium hydroxide at ambient temperature to form hydrated calcium silicates and develop suitable mechanical strength characteristics.

In fact, the pozzolan-lime reaction is also a hydraulic reaction of which the main hydration product is C-S-H gel. It has relatively low mechanical strength, although superiors to those in lime mortars. It has certain capacity of deformation, with low module of elasticity, but, on the other hand, it has low resistance to the adverse climatic conditions. It also presents a scarce presence of soluble salts, and lower permeability to water than lime mortars.

## 2.1 Composition of Cement Phases

The Portland cement is normally constituted by four major phases, according to Balen et al (1999) and Taylor (1990):

- Alite or tri-calcium-silicates:  $3CaO \cdot SiO_2$  ;
- Belite or bi-calcium-silicates:  $2CaO \cdot SiO_2$  ;
- Tricalcium Aluminate:  $3CaO \cdot Al_2O_3$  ;
- Aluminoferrite solid solution or Brownmillerite:  $CaO \cdot Al_2O_3 \cdot Fe_2O_3$  .

Together, the tri- and bi-calcium-silicates comprise 70-80% of the total cement mass. Other phases such as alkali sulphates and calcium oxide are normally present in minor amounts.

### 2.1.1 Alite

Portland cement clinker is composed of between 50 to 70% of Alite, which is basically tricalcium silicate ( $Ca_3SiO_5$ , which in cement chemical nomenclature is expressed as  $C_3S$ ) and can be modified by incorporation of foreign ions ( $Mg^{2+}$ ,  $Al^{3+}$ ,  $Fe^{3+}$ ) in composition<sup>3</sup> and also in the crystal structure<sup>4</sup>, or simply it is a  $C_3S$  solid solution. The Alite is the most important of the constituent phases for initial strength development in normal Portland cements, and reacts quickly with water (Taylor, 1990; Pöllman, 2002; Regourd, 1983).

---

<sup>3</sup> Composition refers to the chemical elements which determines a substance and its particular organization which determines its chemical properties.

<sup>4</sup> Structure chemically refers to both molecular geometry (spatial arrangement of atoms in a molecule and the chemical bonds that hold the atoms together) and to electronic structure (occupation of a compound's molecular orbital).



The  $C_3S$  is formed when the clinker is burned above  $1250^\circ\text{C}$  by a reaction of  $C_2S$  and  $C$ . Also the time of burning and time of cooling after the burning process have an influence in the composition of the Alite (Pöllman, 2002).

### 2.1.2 Belite

Around 15 to 30% of normal Portland cement clinkers are composed by Belite, which is a dicalcium silicate ( $\text{Ca}_2\text{SiO}_4$ ) and also incorporated by some ions and normally present wholly or largely as the  $\beta$  polymorph, or also  $\alpha$  polymorph. However, just the first form has cementing value under normal hardening conditions. Simplifying, Belite is a  $C_2S$  solid solution (Popovics, 1992). The Belite increases the concrete strength at later ages because it reacts slowly with water. By one year, the strength values obtainable from pure alite and pure belite are about the same under comparable conditions (same amount, which do not happen in cements) (Taylor, 1990; Pöllman, 2002; Regourd, 1983).

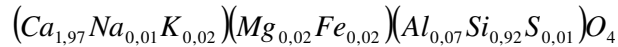
Belite formation is highly influenced by the temperature. Some of the components change drastically with variations of temperature during the burning process of the clinker, as it is stable and readily prepared from reactive  $\text{CaO}$  and  $\text{SiO}_2$  at  $300^\circ\text{C}$ , but at low temperature the  $\gamma$ -belite, or lime olivine is formed, and this form does not hydrate, and is avoided in cement manufacture. On the other hand, Belite can incorporate a larger amount of foreigner ions than the Alite (Pöllman, 2002; Taylor, 1990).

Four forms are known in belite:  $\alpha$ ,  $\alpha'$ ,  $\beta$ , and  $\gamma$ , of  $C_2S$ . But, as already explained, only the  $\beta$  form with a monoclinic unit cell exists in clinker (Ramachandran et al, 2002). Pöllman (2002) explain three different belite origins that can occur in Portland cement clinkers from different sources:

- Primary belite formed by reaction of lime and silicon sources;
- Secondary belite formed by decomposition reaction of alite ( $C_2S + C \rightarrow C_3S$ ) and forming small crystals on the rims of alite crystals;

- Tertiary belite due to the recrystallization of the interstitial phase coming from the decomposition and decreased solid solution of SiO<sub>2</sub> in C<sub>3</sub>A-phases.

Pöllman (2002) describes the composition of belite in Portland cement clinkers as follows:



### 2.1.3 Calcium Aluminate

The calcium aluminate phase in Portland cement clinkers is equivalent to around 5 to 10%, except in sulphate resistant cements where it should be less than 5%. The calcium aluminate is a tricalcium aluminate (Ca<sub>3</sub>Al<sub>2</sub>O<sub>6</sub>) modified by incorporation of foreign ions (Si<sup>4+</sup>, Fe<sup>3+</sup>, Na<sup>+</sup> and K<sup>+</sup>) in composition and sometimes also in structure. Regarding that this component reacts rapidly with water, normally a set-controlling agent (gypsum) is added in order to avoid rapid setting (Taylor, 1990). According to Ramachandran et al (2002) in some clinkers small amounts of calcium aluminate (NC<sub>8</sub>A<sub>3</sub>) may also form.

The most abundant aluminate present in Portland cement clinkers is C<sub>3</sub>A, which can be presented as cubic, orthorhombic or monoclinic symmetry. The orthorhombic and monoclinic solid solutions of C<sub>3</sub>A can be transformed in tetragonal, or pseudo orthorhombic, polymorphs at temperatures above 450°C. On the other hand, the Na-doped (orthorhombic) tricalcium aluminates seem to show decreased reactivity (Pöllman, 2002).

The normal way of crystallization of the C<sub>3</sub>A is as a cubic lattice, but the symmetry can change to orthorhombic and monoclinic point groups due to the incorporation of foreign ions (mainly alkalis and SiO<sub>2</sub>), that can occur in the cements with the permitted proportion of alkalis, according to Pöllman (2002). Moreover, in cubic and in orthorhombic forms the tricalcium aluminates is less vulnerable to sulphate attack (Mehta 1980 apud Popovics, 1992).

Popovics (1992) states that large quantities of tricalcium aluminate in clinker reduces the resistance of the hardened paste against sulphates and other chemical attacks.

#### 2.1.4 Ferrite

Around 5 to 15% of the Portland cement clinkers are formed by a ferrite phase, which is tetracalcium aluminoferrite ( $\text{Ca}_2\text{AlFeO}_5$ ) modified in composition by variation in Al/Fe ratio and incorporation of foreign ions. The reaction with water and the increase of resistance occur in an average between those of alite and belite at later ages (Taylor, 1990). The ferrite phase is responsible for the gray color of the Portland cement regarding to the iron presence. Without iron, its color is white, as in White Cement (Popovics, 1992). It is designated as  $\text{C}_4\text{AF}$  and the potential components of this compound are  $\text{C}_2\text{F}$ ,  $\text{C}_6\text{AF}_2$ ,  $\text{C}_4\text{AF}$ , and  $\text{C}_6\text{A}_2\text{F}$ .

The MgO in the form of crystalline periclase may cause slow expansion, therefore its content in cement is usually limited to 4 to 5%. The same behavior occurs with excessive  $\text{SO}_3$ . Alkalis such as  $\text{K}_2\text{O}$  and  $\text{Na}_2\text{O}$  in excess of 0,6% equivalent  $\text{Na}_2\text{O}$  are not permitted as they promote expansion with certain types of aggregates (Ramachandran et al, 2002).

According to Pöllman (2002) in typical clinkers the uptake of magnesium, titanium and silicon take place, and it is given by the Equation 1:



The same author states that the Portland cement clinkers have low titanium contents which may increase when during the fabrication addition of wastes like painting dusts are added. In this case,  $\text{TiO}_2$ -phases or ilmenite may occur.

### 2.1.5 Minor constituents

The minor constituents of the Portland cement clinker are presented in lower quantities than the other components, but their effects are very important to the behavior of the cement paste.

Regourd (1983) says that the minor phases are constituted by free lime, periclase and sodium and potassium sulphates. Also fillers introduced up to 5% in normalized Portland cements can be calcite or calcite plus dolomite, and can contain minor phases such as quartz and feldspars.

## 2.2 Types of Cements

According to Popovics (1992) all Portland cements have the same constituents and the variations are in the proportions of the components according to their characteristics, which determine the individual type of cement.

The Spanish Standards to cement defines common cements in UNE-EN 197:2000 according to the Table 1.

**Table 1 Types of cements according to UNE-EN 197:2000.**

<b>Type of cement</b>	<b>Denomination</b>	<b>Designation</b>
I	Portland cement	CEM I
II	Portland cement with additions	CEM II
III	Portland cement with high furnace slag	CEM III
IV	Pozzolanic cement	CEM IV
V	Blended cement	CEM V

This is the basic classification of cements. Some of them have subdivisions according to the addition or mixture in the cement. This subtypes can be A, B or C.

The types and subtypes of cements with the respective additions are showed in Table 2 and the additions which can be added to Portland clinker are presented in Table 3.

Table 2 Types and subtypes of cement according to UNE-EN 197:2000.

Type of cement	Subtype	Denomination	Designation
CEM I	No subtype	Portland cement	CEM I
CEM II	A	Portland cement with high furnace slag	CEM II/A-S
	B		CEM II/B-S
	A	Portland cement with Silica Fume	CEM II/A-D
	B		CEM II/B-D
	A	Portland cement with natural pozzolans	CEM II/A-P
	B		CEM II/B-P
	A	Portland cement with calcinated natural pozzolans	CEM II/A-Q
	B		CEM II/B-Q
	A	Portland cement with siliceous fly ash	CEM II/A-V
	B		CEM II/B-V
	A	Portland cement with calcareous fly ash	CEM II/A-W
	B		CEM II/B-W
	A	Portland cement with calcinated slate	CEM II/A-T
	B		CEM II/B-T
	A	Portland cement with limestone L	CEM II/A-L
	B		CEM II/B-L
A	Portland cement with limestone LL	CEM II/A-LL	
B		CEM II/B-LL	
A	Portland cement with all the additions	CEM II/A-M	
B		CEM II/B-M	
CEM III	A	Portland cement with high furnace slag	CEM III/A
	B		CEM III/B
	C		CEM III/C
CEM IV	A	Pozzolanic cement with D, P, Q, V, W	CEM IV/A
	B		CEM IV/B
CEM V	A	Mix cement with S, P, Q, V	CEM V/A
	B		CEM V/B

Table 3 Types of additions according to UNE-EN 197:2000.

Additions	
Denomination	Designation
High furnace slag	S
Silica Fume	D
Natural pozzolans	P
Calcinated natural pozzolans	Q
Siliceous fly ash	V
Calcareous fly ash	W
Calcinated slate	T
Limestone L	L
Limestone LL	LL

The difference between Limestone L and LL is the total organic content. The sulphates resistant cements are standardized by the UNE 80303:2001 and classified according to Table 4.

**Table 4 Sulphate resistant cements according to UNE 80303:2001.**

Type	Denomination	Subtype/ Designation	Specification of the clinker		
			C <sub>3</sub> A %	C <sub>3</sub> A + C <sub>4</sub> AF %	
I	Portland cement sulphate resistant	I	≤ 5	≤ 22	
II	Portland cement with sulphate resistant additions	With High furnace slag (S)	II/A-S II/B-S	≤ 6	≤ 22
		With Silica Fume (D)	II/A-D		
		With Natural pozzolans (P)	II/A-P II/B-P		
		With Siliceous fly ash (V)	II/A-V II/B-V		
III	Cements sulphate resistant with additions	With High furnace slag (S)	III/A III/B III/C	≤ 8	≤ 25
		Pozzolan cements (D+P+V)	IV/A IV/B	None	None
		Composed Cements (S+P+V)	CEM V/A CEM V/B	≤ 6	≤ 22
V			≤ 8	≤ 25	

### 2.3 Hydration mechanisms

Since the cement is composed by several different phases, as described before, in contact with water each of this composites reacts in a different way. The final result is a resistant mass solid and dense. The reactions occur in different times and velocities, dissolving slowly the cement particle and forming the hydrated phases (Mehta and Monteiro, 2004).

The hydration process is exothermic, i.e. releases heat during the process. This heating of the system will accelerate the reactions, and the total heat generated during the process show the cement hydration evolution. C<sub>3</sub>A is the most reactive phase, influencing directly at the workability of the paste and consuming a high amount of water during the hydration (Kirchheim, 2008).

Kirchheim (2008) presented a compilation of Scrivener and Bishop works to show the hydration process related to heat process and the products formation. This graph is presented in Figure 2.

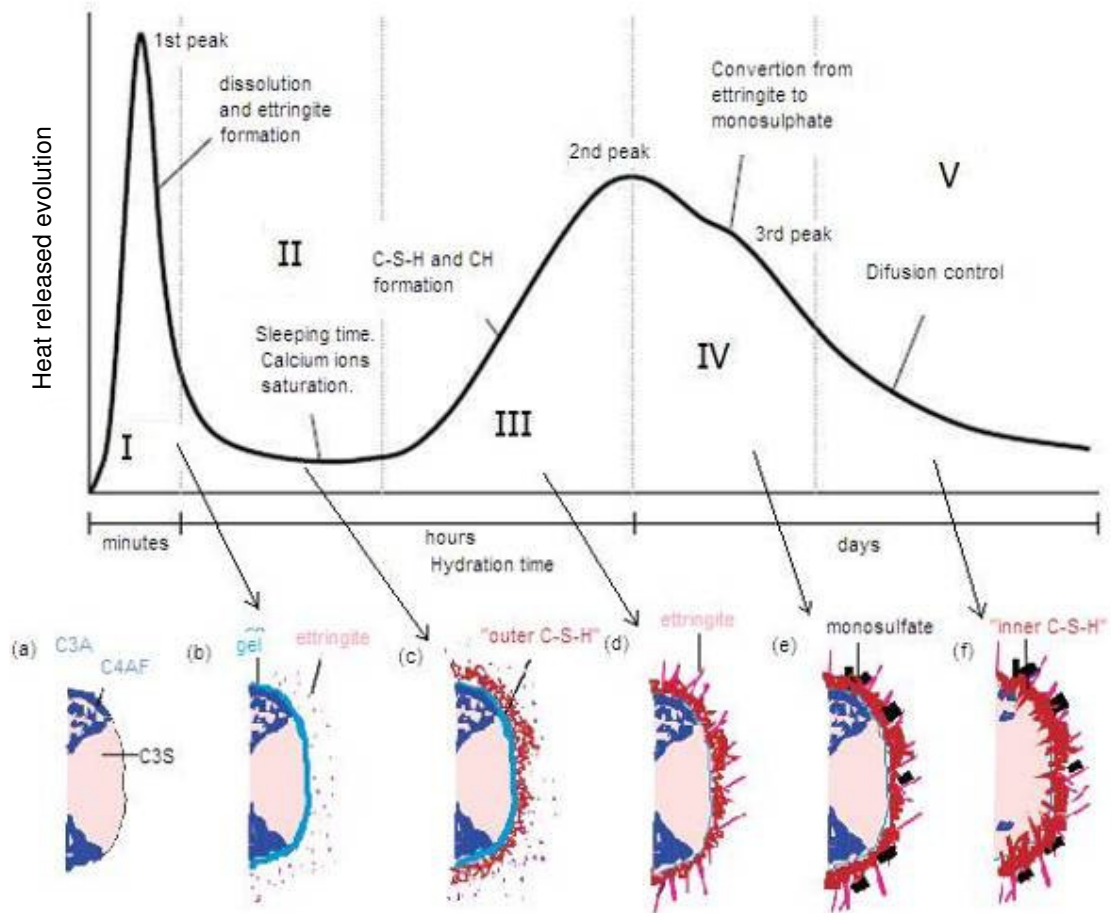
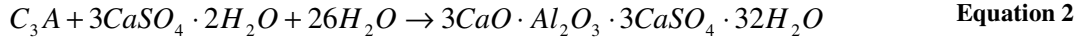


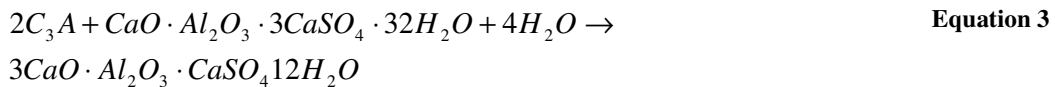
**Figure 2** Graph of hydration stages and schematic representation of anhydrous cement particle. At the graph, I represents the beginning of the heat evolution regarding to the partial dissolution of the cement and beginning of C<sub>3</sub>A and C<sub>3</sub>S hydration. II represents the induction or sleeping period, with low heat release, indicating the C<sub>3</sub>A hydration control. III shows the retaking of the reactions and increasing of heat. IV represents the reduction in the quantity of sulphate ions. In the drawings, (a) shows the anhydrous cement particle, (b) presents the effect after around 10 minutes, (c) after 10 hours, (d) after 18 hours, (e) after 1-3 days and (f) after 2 weeks. (Kirchheim, 2008 - compilation from Scrivener, 1984 and Bishop, 2003).

After the contact with the water, ions start to be dissolved, including the calcium sulphate, until the saturation. After that, the anhydrous phases C<sub>3</sub>S, C<sub>3</sub>A e C<sub>4</sub>AF start to dissolve forming small ettringite needles around the cement grain (Bishop, 2003; Kirchheim, 2008), following the Equation 2 (Schmidt, 2007). A C-S-H (Calcium

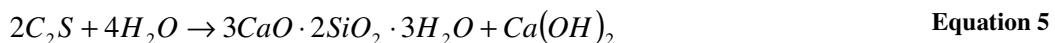
Silicate Hydrated) gel forms, provoking an exothermic peak, showed in stage I of the scheme above.



After this fast period, a slowdown on the  $C_3A$  formation occurs because of the ettringite covering the grain, starting the sleeping period (stage II), which depends on the quantity of sulphates in the clinker. Finishing the added sulphate by the abstention of limestone, it starts to form monosulphate from the ettringite and  $C_3A$  available, Equation 3 (Schmidt, 2007, Kirchheim, 2008).



When the C-S-H gel is destroyed, the sleeping period finishes,  $C_3S$  and  $C_2S$  react to form C-S-H phases and portlandite, with  $C_3S$  forming more portlandite, according to the following equations (Schmidt, 2007, Kirchheim, 2008). The heat releasing increase again (stage III). The final setting time occurs during this period and the hardening of the cementitious system starts.



The ettringite is converted in calcium trissulfoaluminate hydrated by the reaction with ions  $Al^{3+}$  starting the stage IV. The ions remaining form a protection around the grain with the  $Ca^{2+}$ , starting the stage V (Kirchheim, 2008).



Juenger, Monteiro and Gartner analyzed the early hydration of clinkers with Soft X-Ray transmission microscopy and presents the following figure, where the cement grain hydration can be visualized.

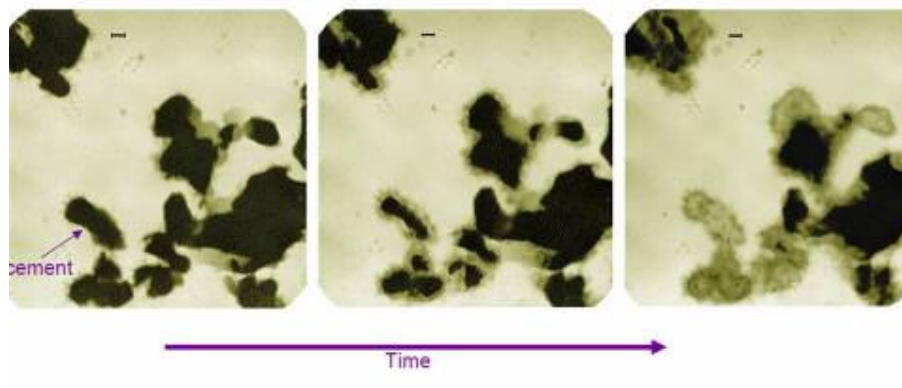


**Figure 3** Cement hydration (Source: M. G. Juenger, P. J. M. Monteiro, E. Gartner. UC Berkeley, and G. Denbeaux, LBNL).

The products formed by  $C_3S$  and  $C_2S$  hydration are similar, but the velocity of the reactions are different (Taylor, 1990).

## 2.4 Hydration products

The principal product of the cement hydration is the C-S-H, formed rapidly by the hydration of alite and slowly by the hydration of belite. The C-S-H will provide resistance and durability for the cementitious system. It is an amorphous composite, with a Ca/Si relation varying along the time (Sanz, 2007).

The Calcium hydroxide (CH) is formed mainly from alite hydration, using the excess lime from the C-S-H formation to hydrate the alite and form CH.

Moreover, ettringite is an hydration product, present as rod-like crystals in the early stages of cement hydration.

Finally, monosulphate tends to occur in the later stages of hydration, after a few days. Usually, it replaces ettringite, either fully or partially. Both ettringite and

monosulphate are compounds of  $C_3A$ ,  $CaSO_4$  (anhydrite) and water, in different proportions.

## ***2.5 Influence of Silica Fume addition***

Silica fume is a by-product of the manufacture of silicon and ferrosilicon, where escaping gaseous SiO oxidizes and condenses as amorphous silica ( $SiO_2$ ). It was originally introduced at concrete as a pozzolana, but its action is not only that of a very reactive pozzolana but also reactive in other respects. On the other hand, it is a very expensive product (Neville, 1995).

Silica in the form of glass is highly reactive, and the smallness of the particles speeds up the reaction with calcium hydroxide produced by the hydration of Portland cement. Due to this small particle size, it can enter the spaces between the particles of cement, providing the packing of the system, and increasing the resistance and durability (Neville, 1995).

The reaction between silica fume and CH formed during the hydration of Portland cement starts practically immediately after the mixing. With additions between 15 to 20% by mass of CH is completely consumed in about 28 days under certain conditions. It provokes the maintenance of the pH of the porous solution above 12,7, or above the CH saturated solution value. C-S-H with Ca/Si molar ratio estimated to be about 1,0 is formed as a product of the reaction between silica fume and CH, exhibiting a higher degree of condensation rather than the C-S-H phases which are richer in CaO and as a result its content of chemically combined water is lower (Locher, 2006).

In this research the silica fume was used to be a source of silica to the formation of thaumasite.

### 3 DURABILITY

Taylor (1990) describes that concrete is an extremely durable material if it is properly designed and produced for the environment in which it has to serve. If not, it may deteriorate. Any type of concrete can be durable in some environments.

According to Neville (1995), the term durability is related to the capacity of a structure to continue to perform, during its expected service life, its intended functions, maintain its required strength and serviceability, against deterioration process. Moreover, maintenance is always necessary to be done, regarding to allow this expected service life.

The durability of the cementitious materials is a function on several factors such as type and composition of cement, aggregates, mix water, compaction, admixtures, and reinforcement, The degradation of the cementitious materials can result from a property of any of its constituents, reaction between its constituents, poor compaction, etc. In addition, other degradation factors such as weathering or environment reaction can also act on the cementitious material and affect its durability (Oberholster et al., 1983).

Many of the monuments built in the 19<sup>th</sup> and 20<sup>th</sup> century were constructed using modern hydraulic mortars, such as hydraulic lime, pozzolan and cement-based. On the other hand, monuments need restoration to conserve their characteristics, and in Europe similar hydraulic mortars have been used in treatments carried out during last and the present century for this propose. Regarding to this fact, is essential to understand their durability for planning future conservation treatments on the built heritage (Cassar, 2001).

It is known that  $\text{SO}_2$  is the main component of pollution that cause damage to hydraulic mortars, which is the most sensitive building material, because of the formation of primary and secondary damage products, such as ettringite and thaumasite (Cassar, 2001).

### 3.1 Carbonation

The environment where the structures are inserted contains CO<sub>2</sub> which, in presence of moisture, reacts with hydrated cement paste, most readily with Ca(OH)<sub>2</sub>, producing CaCO<sub>3</sub>. The rate of carbonation in concrete or mortars increases with an increase in concentration of CO<sub>2</sub>, especially in high water/cement ratio, being transported through the porous system. The concentration of CO<sub>2</sub> in the air vary from 0.03% by volume in rural area, passing to 0.1% in unventilated laboratory, until large cities where it arise 0.3% and in exceptionally in some cases up to 1% (Neville, 1995). The carbonation process occurs slowly following the Equation 6.



Carbonation itself do not cause deterioration of concrete or mortar, but cause carbonation shrinkage, exposing it to the entrance of aggressive agents, and reduces the pH of the pore water in hardened Portland cement paste from between 12.6 to 13.5 to a value of about 9, when all the Ca(OH)<sub>2</sub> present at the paste is carbonated, this value decreases to around 8.3. At reinforced concrete it is a problem because it allow the corrosion of the steel (Neville, 1995). However, in historical concrete and mortar without reinforcement, the important factor is the shrinkage and the formation of phases that would allow also the formation of thaumasite-object of this research.

The carbonation occurs progressively from outside to inside of the exposed surface, but in a decreasing rate since the CO<sub>2</sub> has to diffuse through the pore system. The rate of carbonation depends on the moisture content of the system. The diffusion is a slow process if the pores in hydrated cement paste are filled with water (CO<sub>2</sub> diffusion in water is 4 times slowly than in air). Moreover, if there is no sufficient water inside the pores, CO<sub>2</sub> remains in gas form and does not react with the hydrated cement. The highest level of carbonation occurs when the relative humidity is between 50 and 70% (Neville, 1995).

On the other hand, when carbonation occurs, CaCO<sub>3</sub> could occuppies a greater volume in the paste than the previous composite Ca(OH)<sub>2</sub>, reducing the paste porosity

and aiding the hydration of the hitherto unhydrated cement particles. It provides a hardening and strengthening of the paste surface, and reduces the permeability, moisture movement and, consequently, increases the resistance to the forms of attack that are controlled by the permeability (Neville, 1995).

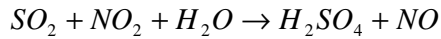
### ***3.2 Sulphate Attack***

Some of the cultural heritage in different countries are located in big cities, several times exposed to aggressive environments, close to industry areas or to polluted city centers, and regarding of that it can be submitted to sulphate atmosphere. Colleparidi (2003) classify the deterioration process according to origin of the sulphate:

- Deterioration by external origin sulphates: the sulphates are originated at the exposition environment, such as sulphate contaminated soil or sulphate aggressive water;
- Deterioration by internal origin sulphates: the sulphates have origin in the concrete or mortar, for contamination or sulphate excessive addition at the constituent materials. For example, the utilization of recycled aggregates polluted by sulphates, or sulphates provided by clinkerization with alternative fuel rich in sulphur (Mehta & Monteiro, 1994).

Regarding to the external origin, Palomo et al underlines that during the last decades the problem of the acid rain has acquired serious dimensions, and also affecting historical buildings. The pH of the rain uses to be between 4 and 4,5, and its acidification is due, in principle, to the effect of the  $\text{HNO}_3$  and the  $\text{H}_2\text{SO}_4$ , formed for reaction of  $\text{SO}_2$  and  $\text{NO}_2$  with the water. When in contact with the mortar and concrete this acid water give place to the formation of calcium nitrates, sulphates, bicarbonates, among others.

$\text{SO}_2$  is one of the most dangerous atmospherical pollutants while there is a strong synergy effect produced by  $\text{SO}_2$  and  $\text{NO}_2$  when they are together, as can be seen in the following equation:



**Equation 7**

The same authors underline that the chemical reaction of  $SO_2$  with the cement mortar components is 35 times faster in presence of water and an oxidant element than in absence of those elements; while it is two order of magnitude quicker if the reaction takes place between  $SO_2$  and lime mortar phases.

The desegregation of the concrete or mortar, as a result of chemical reactions between hydrated Portland cement and sulphate ions, have two different forms depending on the concentration and source of the sulphate ions at cement water and the cement past composition: as a concrete expansion, with crack and enlargement of the permeability resulting in facilities to aggressive water penetration, or as a progressive lose of resistance and mass because of the deterioration and lose of cohesion of the cement products (Neville, 1995).

The degradation can be due to different types of sulphates such as sodium sulphate ( $Na_2SO_4$ ), ammonium sulphate ( $(NH_4)_2SO_4$ ), magnesium sulphate ( $MgSO_4$ ), calcium sulphate ( $CaSO_4$ ), sulfuric acid ( $H_2SO_4$ ), among others. Just barium sulphate and lead sulphate are not aggressive to cementitious systems (Oberholster et al, 1983).

The performance of cementitious systems regarding to the sulphate attack is influenced by its physical properties such as permeability, diffusion, porosity, and the availability of the moisture, differential water pressure, temperature and temperature gradient. In cases when the sulphates attack the hydrated calcium silicates directly, (principal binders) the concrete will deteriorate, lose strength and eventually disintegrate. On the other hand, in cases where the attack is on the hydrated calcium aluminates the expansion is usually the main cause, but the mechanism whereby the concrete deteriorates is not always very clear (Oberholster et al, 1983).

Based on this, the intervenient factors to sulphate attack occurrence are:

- Quantity and nature of the present sulphate: The sulphate attack just occurs when the sulphate concentration is higher than a threshold limit. Above this limit the velocity of the attack increase with the solution concentration, but with higher than 0,5% of  $MgSO_4$  or 1% of  $NaSO_4$

concentrations the increase on the velocity is lower (Neville, 1995). In addition, the type of sulphate is important for the reaction, since the velocity of attack depends on the reposition velocity of the sulphate removed by the reaction with the cement;

- Water flux and seasoned variation: The process is fastest when a side of the structure is exposed to sulphate water pressure. The alternate saturation and dryness result in accelerated deterioration. Besides that, the conditions are most severe when the concrete or mortar is completely buried (Mehta & Monteiro, 1994).
- Concrete quality: If it is impossible not to permit the sulphate water to reach the concrete, it is necessary to control the concrete by providing a low permeability. Nevertheless in historical constructions it is impossible to provide this low permeability without reconstruct the affected element (Mehta & Monteiro, 1994).
- Thermal cure historic: normally this deterioration mechanism is attributed to intern sulphates attack. The thermal decomposition of ettringite occurs when the concrete or mortar is subjected to temperatures higher than 80°C. The ettringite decomposition is the principal cause of internal sulphate deterioration, followed by high SO<sub>3</sub> cement content (Taylor, 1997).

It is known that high alumina content in Portland cement provides low sulphate resistance for the system. Based on this information, the sulphate resistant cement was developed, reducing the amount of Al<sub>2</sub>O<sub>3</sub>. One example is the cement type V in ASTM classification, with lower than 5% C<sub>3</sub>A content, that can resist to moderate conditions of sulphate. In addition, it is possible to reduce the Ca(OH)<sub>2</sub> of the hydrated cement past using cements with some additions, such as pozzolan, to react with this compost and avoid it to be available to react with the sulphate. However, in historical buildings it is impossible to use these techniques without reconstruct the affected area. Hence, it is necessary to find some alternative to reduce the concrete and mortar permeability and reduce the damage by sulphate attack (Oberholster et al., 1983).

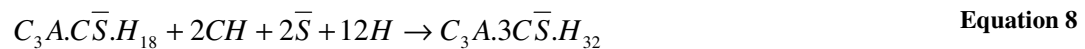
Sometimes, other complex sulphates and carbonates are found in deteriorated cementitious systems, such as thaumasite and solid solutions of thaumasite and ettringite, in situations where sulphate attack is associated with excess carbonation. This phenomenon is the object of this work and will be presented in detail later.

### 3.2.1 Mechanism of attack

The attack on the cementitious system may occur in two different ways: delayed ettringite formation or gypsum formation. Nevertheless, in cementitious systems with a source of carbonate the formation of thaumasite can be observed.

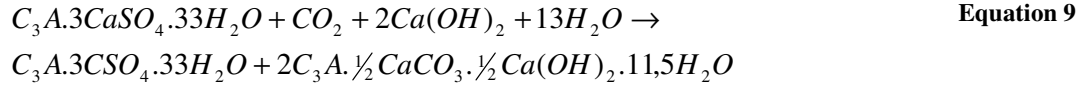
#### 3.2.1.1 Delayed ettringite formation

When the cement paste are in contact with sulphate ions the alumina hydrates, in reaction with calcium hydroxide, are converted in later ettringite, which is a highly sulphated compound. This reaction occurs at hardened paste causing heterogeneous expansion and deterioration. One of the principal factors for the formation of that compound is the  $SO_4^{2-}/Al_2O_3$  relation: when it is low, there are monosulphoaluminates ( $C_3A.C\bar{S}.H_{18}$ ) presence, allowing their transformation in ettringite ( $C_3A.3C\bar{S}.H_{32}$ ) again because of the raise of  $SO_4^{2-}$  as a consequence of sulphate ions from external or internal sources, as showed in Equation 8.



Furthermore, Taylor (1997) defends that this reversion can occur because of the presence of other ions such as  $CO_2$  (Equation 9), forming ettringite and carbonating the paste.



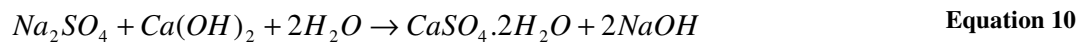


The sources of reactive aluminum are AFm phases (monosulphate, monocarbonate) and calcium aluminate originating from the clinker phases (C<sub>3</sub>A and C<sub>4</sub>AF) (Schmidt, 2007).

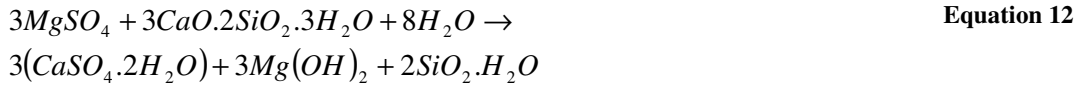
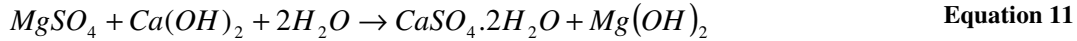
At levels of pH between 10.5 and 13.0 in pure systems, the ettringite is stable, and have this characteristics in cement systems at pH up to 14, starting to decompose in pH lower than 10.5 (Mehta, 1983).

### 3.2.1.2 Gypsum formation

The gypsum formation as a result of cation exchanging also can provoke expansion. The hardened paste deterioration by the gypsum formation occurs in a process where the rigidity and resistance are decreased, followed by expansion and fissuration and finally transforming the system in a friable and even soft mass, regarding that the C-S-H phase decalcification. Depending on the type of cation at sulphate solution (Na<sup>+</sup> or Mg<sup>2+</sup>) the calcium hydroxide or the C-S-H can be transformed in gypsum by sulphate attack, that is an important factor for the durability of the cement system in a sulphate exposure, as illustrated in Equation 10 to 12 (Mehta and Monteiro, 1993).



In this case of sodium sulphate attack, the sodium hydroxide formation as a sub product of the reaction assures the system alkalinity, which is essential for the C-S-H stability.



In the case of magnesium sulphate attack, Equation 11 and 12, the conversion of calcium hydroxide in gypsum is followed by magnesium hydroxide relatively insoluble and few alkaline. With this, the C-S-H stability in the system is reduced and attacked by the sulphates. Thus, magnesium sulphate attack is more severe in concrete and mortar.

Schmidt (2007) underlines that minimizing the amount of portlandite in the hydrated cement paste increases the resistance of gypsum formation since gypsum can be a source of sulphate for the formation of AFt phases, such as ettringite and thaumasite.

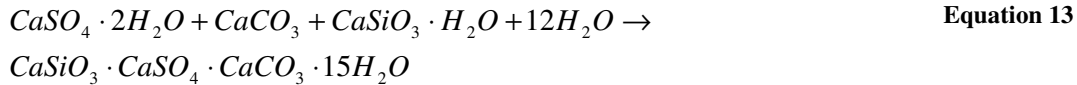
### 3.3 *Thaumasite*

In 1965 decayed concrete and repairing mortars used for the conservation of the architectural heritage presented thaumasite formation, identified for the first time, but nowadays the formation process of thaumasite is still not been explained (Balén et al, 1999).

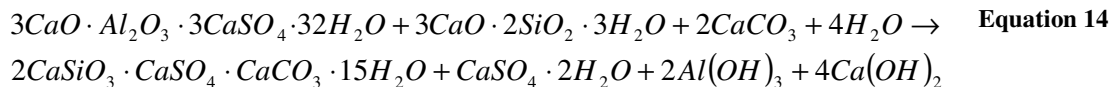
Thaumasite by sulphate attack (TSA) is more serious than common types of deterioration associated with sulphates, regarding that because the main calcium silicate cementing phases are affected, rather than only the portlandite and calcium aluminate phases, causing loss of integrity and strength (Sims and Huntley, 2004).

Thaumasite is a calcium silicate carbonate sulphate hydrate that can be found among the deterioration products of cementitious materials with ettringite, gypsum or on its own. It can be formed through a combination of sulphate attack and carbonation, and occur in concrete structures and in masonry walls of historic buildings. Thaumasite formation causes damage to cementitious materials by decomposing the C-S-H phase.

The formation of this compound can follow the Equation 13 (Ramachandran et al, 2002; Balen et al, 1999; Crammond, 2002).



In addition, Schmidt (2007) describes the thaumasite formation directly from ettringite, which reacts with C-S-H, carbonate,  $Ca^{2+}$  ions and water, called “Woodfordite-route”, following the Equation 14.



Woodfordite is a solid solution whose end members are ettringite and thaumasite. Bensted (2003) underlines that this type of thaumasite just occurs in cement systems exposed for long time to temperatures lower than 2°C. This reaction is very slow to begin, but once thaumasite has started to form the rate of reaction appears to rise significantly, being the woodfordite route relatively quicker than the direct route. Both alite and belite form the C–S–H binder, whilst aluminate and ferrite with gypsum contribute to thaumasite formation via the woodfordite route.

At cementitious systems subjected to sulphate attack the direct and woodfordite routes are interdependent, regarding that the presence of ettringite as a starting material is essential for the woodfordite route. Direct thaumasite formation affects the alite and belite phases, while the woodfordite route affects all four principal Portland cement phases: alite and belite for the C–S–H which gradually engulfs the ettringite, and aluminate and ferrite by forming the ettringite in the first place (Bensted, 2003).

Taylor (1990) describes that crystal structure and morphology of thaumasite resemble those of ettringite ( $C_3A \cdot 3CaSO_4 \cdot 32H_2O$ ), and Balen et al (1999 p. 4) relates that these have a very similar X-ray diffraction pattern, which will be discussed at Item 3.3.2, and are frequently found together. In the past, regarding on this fact, several times the thaumasite had been identified as ettringite, which has been considered by a great

number of authors to be the only cause of the degradation of concrete and mortar in the presence of sulphates. The differences in this case are in the octahedrally coordinated structure of silicon in thaumasite that normally has a tetrahedral structure. In addition, aluminum is octahedrally coordinated in ettringite and in thaumasite could be replaced by silicon and consequently form a continuous solid solution. At thaumasite, the alumina at ettringite is replaced by silicon and the carbonate partly substitutes the sulphate, as illustrated in Figure 4.

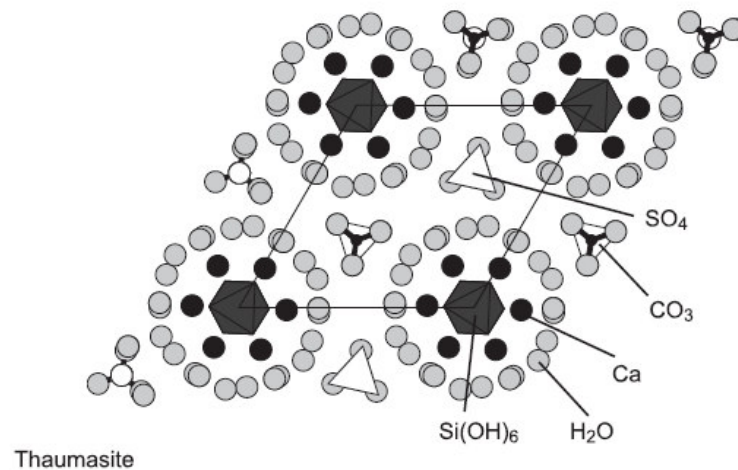


**Figure 4 Crystal structure of thaumasite—projection on a – b plane (Torres et al, 2004).**

According to Macphee and Diamond (2003) the thaumasite is an ettringite analogue. It contains silicate ions that fill the sites where normally had aluminate, and carbonate ions in places associated with sulphate ions, so it is an AFt<sup>5</sup> compound. It can happen as a minor secondary reaction product in concrete, without provoke severe deteriorations.

However, as described by Collepardi (1999) both thaumasite and ettringite provoke expansion, cracking, spalling, loss of strength and adhesion of cementitious materials, but ettringite formation is associated primarily with expansion, cracking and spalling, while thaumasite formation provokes more severe damaging, transforming hardened concretes or mortars in a pulpy mass because of the loss of strength.

<sup>5</sup> AFt is aluminate-ferrite-mono hydrate phase ( $\text{Al}_2\text{O}_3\text{-Fe}_2\text{O}_3\text{-tri}$  phases). The most important AFt phase is ettringite, and when determined cations in AFt phases replace the  $\text{Ca}^{2+}$  or  $\text{Al}^{3+}$  or both, other components such as thaumasite are formed (Taylor, 1990).

Crammond (2002) observes that the expansive disruption is not a characteristic feature of the thaumasite formation, just occur in some cases. An example of the thaumasite formation is presented in Figure 5.

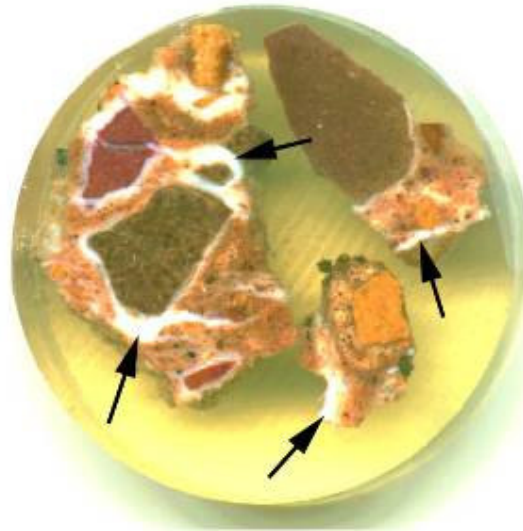


**Figure 5 Polished section of degraded concrete from a highways structure in the United Kingdom. Thaumasite has formed around coarse limestone aggregate (large dark particles) and in cracks. Examples of thaumasite are arrowed. This polished section was 40mm in diameter but thaumasite formation is so extensive that it requires little magnification to be clearly visible (Source: [www.understandin-cement.com](http://www.understandin-cement.com)).**

On the other hand, Crammond (2002) describes two different ways in which thaumasite can precipitate as a reaction product, especially within concretes and mortars:

- TSA: thaumasite form of sulphate attack, when there is a significant damage to the matrix of a concrete or mortar as a consequence of replacement of cement hydrates by thaumasite; as a consequence, concrete turns into a soft, mushy mass with a distinctive white coloration;
- TF: thaumasite formation, where thaumasite can be found in pre-existing voids and cracks without necessarily causing deterioration of the host concrete or mortar.

Macphee and Diamond (2003) underlines that “TSA deterioration can be much more severe than conventional forms of sulphate attack as it is associated with the

deterioration of the calcium silicate hydrate (C–S–H) gel, the main binding phase of the cement”.

Regarding to TSA, it was initially thought that the formation process could be inhibited by using sulphate-resistant cement, which contains low  $C_3A$  content, although the Thaumaside Expert Group (1999) found high quality concrete made with sulphate-resistant cement affected by TSA, as it still contain similar calcium silicate phases and are thus not immune to TSA (Sims and Huntley, 2004).

Blanco-Varela et al (2006) presents a review about some researches developed by different authors about comparing TSA formation in concretes and mortars made with sulphate-resistant cements, and there is a consensus that TSA also forms in specimens made with common cement but the rate of formation is slower than in specimens with sulphate-resistant cements. It occurs because normal sulphate attack usually results in the formation of ettringite using aluminium provided by the cement which is limited in quantity in normal concrete. On the other hand, the thaumasite formation does not involve aluminium, but if it is given an adequate supply of sulphate and carbonate, thaumasite can continue to form until the calcium silicate hydrate present on the cementitious system is completely decomposed. Consequently, while the use of sulphate-resisting Portland cement provides some defense against normal sulphate attack, it does not give any particular protection against thaumasite formation. These authors underline that the  $C_3A$  content of the cement affect the type of expansive salt produced and its formation process, according to observed an their results, showing that magnesium sulphate is less aggressive and form more TSA in low  $C_3A$  cement specimens than gypsum sulphate.

The same authors say that the gypsum contained in sulphate-resistant cement affords a sufficient supply of sulphates to form thaumasite, so it is not necessary additional or external source of these ions. In this case, the process of formation is very slow but extremely destructive.

Sibbick and Crammond (2003) say that TSA develops within hardened concrete through four progressive stages of degradation (zones 1–4), presented in Figure 6.

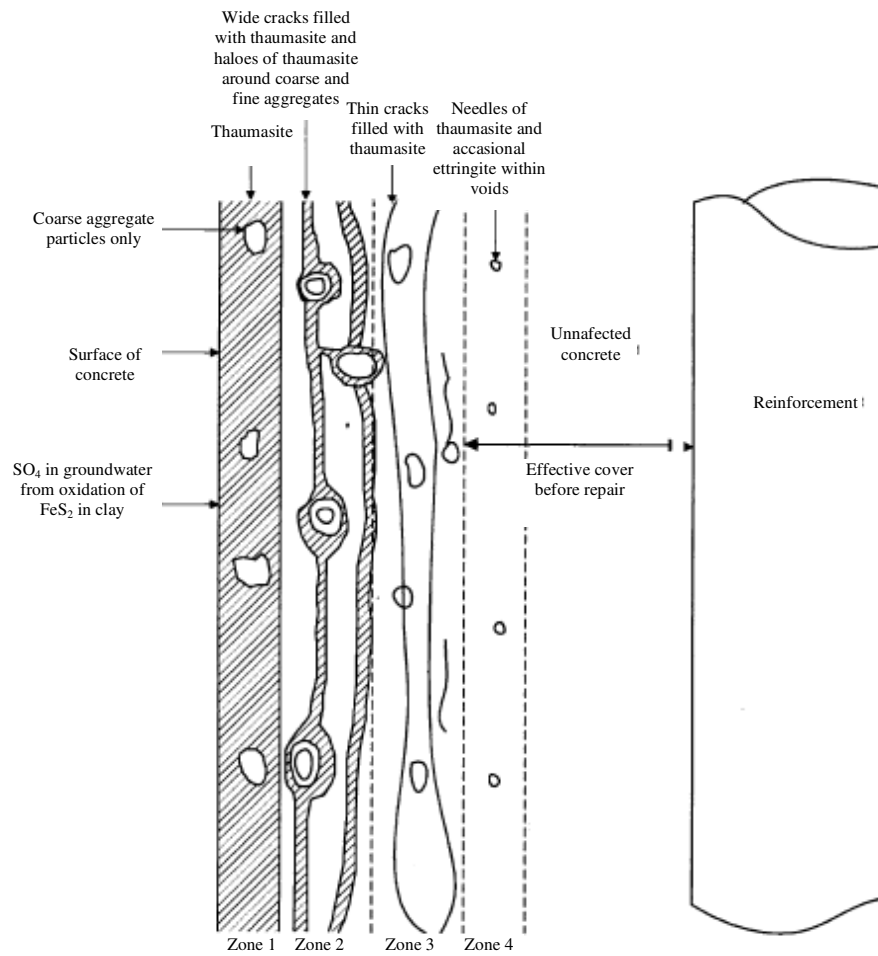


**Figure 6 Sketch of the idealized form taken by TSA degradation with high quality structural concrete (Sibbick and Crammond, 2003).**

The simple four-stage degradation sequence for TSA development described for the authors related to the Figure are:

- Zone 1: No visual evidence of attack; petrographic examination can reveal occasional voids and adhesion cracks around aggregate particles lined with thaumasite or ettringite;
- Zone 2: Thin cracks lined with white thaumasite begin to appear running sub-parallel to the concrete surface. Calcium carbonate is sometimes precipitated into these cracks. Little portlandite is observed within the cement paste matrix. There is no evidence of other sulphate-bearing minerals;

- Zone 3: An abundance of sub-parallel cracks filled with thaumasite become wider and the amount of unattacked cement paste matrix is greatly reduced. Haloes of white thaumasite can be seen around coarse and fine aggregate particles. Calcium carbonate is sometimes precipitated into the cracks. Little portlandite is observed in the still unattacked cement paste. There is no evidence of other sulphate-bearing minerals;
- Zone 4: Complete transformation of the cement paste matrix to thaumasite. All that remains are occasional aggregate particles embedded in extremely soft white mush (thaumasite) and a few residual 'islands' of heavily depleted cement paste.

### 3.3.1 Formation conditions

At low temperatures, between 1 to 4°C, thaumasite can be produced since gypsum and calcium carbonate can interact with CaO and SiO<sub>2</sub> or Ca<sub>3</sub>SiO<sub>5</sub> or Ca<sub>2</sub>SiO<sub>4</sub> when the water is present. Another form of formation of thaumasite is through the reaction of Ca(OH)<sub>2</sub>, CaCO<sub>3</sub> and amorphous silica with gypsum (Balen et al, 1999).

However, Sims and Huntley (2004) say that TSA can occur at higher temperatures, including ambient temperatures in Mediterranean-type climatic regions. In this cases, the rate of reaction may be slower or accelerated by factors other than temperature.

Hobbs (2003) underlines that thaumasite normally forms at leached, surface near regions of the concrete.

According to Collepardi (2003) the external sulphate attack damage occur predominantly, and one of them form the thaumasite, when the sulphate attack happen on C-S-H and CH in the presence of carbonate ions.

Crammond (2002) affirms that all the components to comprise the thaumasite (sulphate ions, carbonate ions and calcium silicate or calcium silicate hydrate) must be available in the materials themselves or be transported to the reaction site by water. Based on this fact, Collepardi (1999) says that almost all the historic buildings have water presence, which can come from rain water or capillary rising water from the



foundations in contact with wet grounds, which can rise as high as 15 m in some cases, but normally due to the water evaporation, the capillary rise is at most approximately 2 m in walls with a porous mortar rendering layer or without a rendering mortar. As the water presence is necessary to the thaumasite formation, it is an important factor to be considered.

The formation of thaumasite occurs in pH higher than 12,5, and decreases at pH lower than 8,0 (Hobbs and Taylor, 2000). In addition, gypsum is needed for this formation, as well as for ettringite's formation. It can be present in historic buildings for one of the following reasons (Collepari, 1999):

- used as binder for gypsum mortars in the original construction or in the later repair of the buildings;
- by the reaction of sodium or magnesium sulphate from bricks with lime or C-S-H in jointing or rendering mortars;
- in situ by reaction of SO<sub>2</sub> with oxygen, water and lime or calcite of the surface mortar;
- by reaction of sulphate ions in capillary rise water with lime or C-S-H of the cementitious materials in the wall.

On the other hand, Crammond (2002) shows that carbonate ions are not required to form ettringite or gypsum but are necessary to form thaumasite. It can be provided by carbon dioxide dissolved in water, or it can be derived from limestone present within the building material itself as aggregate or filler. With this, if a cementitious material which contain limestone comes into contact with sulphated water, all the components necessary for thaumasite formation are present. The velocity of the reaction increases considerably at cold temperatures below 15°C, and the mixture needs high amount of water.

Nevertheless, Blanco-Varela et al (2006) says that mortar carbonation provides sufficient carbonates for the process to occur and defends that calcite addition decrease the thaumasite formation when high C<sub>3</sub>A content cement is used.

According to Collepari (1999) the type of sulphate salt which attack the cementitious materials is not a condition for the thaumasite formation consuming C-S-H, differently on the ettringite formation.

Juel et al. (2003) developed a model based on the phase rule to predict the hydrate phase mineralogy and phase proportions from the chemical composition of hydrated Portland cement altered by sulphate attack. The model predicts, among other things, that thaumasite, which forms at low temperature, is unstable in the presence of AFm phases, and can only form in systems that would otherwise form gypsum at higher temperatures. The result of this model is shown in Figure 7 for a mixture of Portland cement and 15 wt.% raw feed precipitator dust (calcite). Thaumasite is assumed to be a stable phase in the example given corresponding to reaction at low temperature (lower than 15°C). Gypsum forms instead when all the available  $Al_2O_3$  has reacted with sulphate to form ettringite.

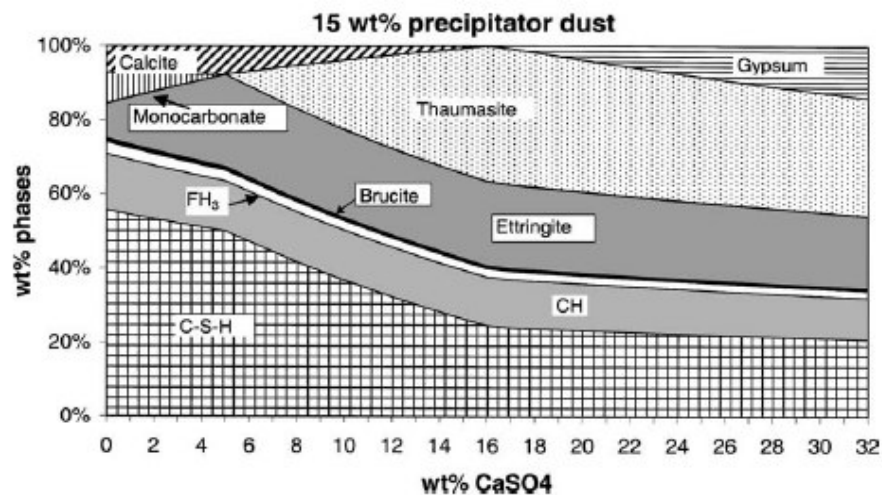


**Figure 7** The phase composition of a blended cement with 15 wt.% raw feed precipitator dust shown as a function of the  $CaSO_4$  content. Thaumasite is assumed to be a stable phase (Juel et al., 2003).

The figure shows that an addition of about 5 wt.%  $CaSO_4$  is required for initial thaumasite formation to occur. The addition of about 17 wt.%  $CaSO_4$  is necessary to form gypsum in the presence of thaumasite (Juel et al., 2003). It is evident the incompatibility of the thaumasite with Monocarbonate, gypsum and calcite, but for a

better visualization, the authors suggest a simplified ternary sub-system, presented in Figure 8.

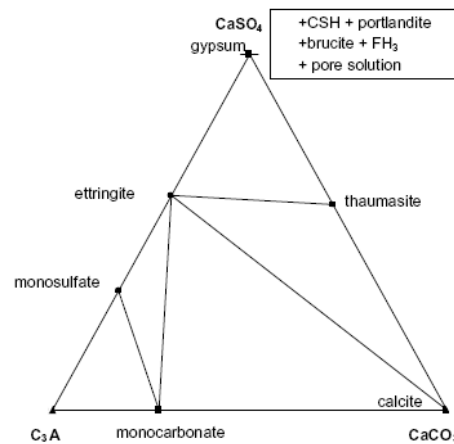


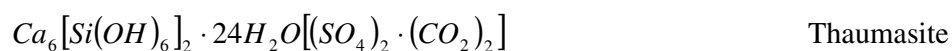
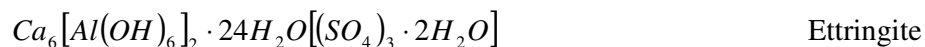
**Figure 8** Projection of the relevant phases on to sub-ternary compatibility diagram for the  $C_3A$ - $CaCO_3$ - $CaSO_4$  system showing the relative contents of the phases (Juel et al., 2003).

It shows that thaumasite can only form at sulphate contents necessary to form gypsum at higher temperatures (above the ettringite - calcite tie-line). Unlike the situation at high temperature, calcite and gypsum cannot coexist in the presence of thaumasite. It is also evident that  $Al_2O_3$  rich systems (the one that contain fly ash or slag) tend to be most resistant to thaumasite related damage since higher contents of sulphate would be required to form thaumasite. It also shows why sulphate resisting Portland cement should be least resistant (Juel et al., 2003).

### 3.3.2 Identification

The formation of TSA will transform the cement paste matrix in a white mush composed of thaumasite, which loosely holds the surrounding aggregate particles together. In addition, it will form sub-parallel cracks filled with thaumasite and white haloes of thaumasite occurring around aggregate pieces. It can also occur in a non-destructive way, as mentioned before, by the TF (Crammond, 2002).

On the other hand, according to Collepardi (1999) the crystallographic structure of ettringite and thaumasite is very similar, in spite of the difference between their chemical composition:



Consequently, the X-Ray diffraction patterns for this two composites are very similar because of the close similarity in unit cells and low-angle, high-intensity reflections (Skibsted et al., 2003 p. 823), as illustrated in Figure 9, although this technique is the most commonly used for detection of thaumasite.

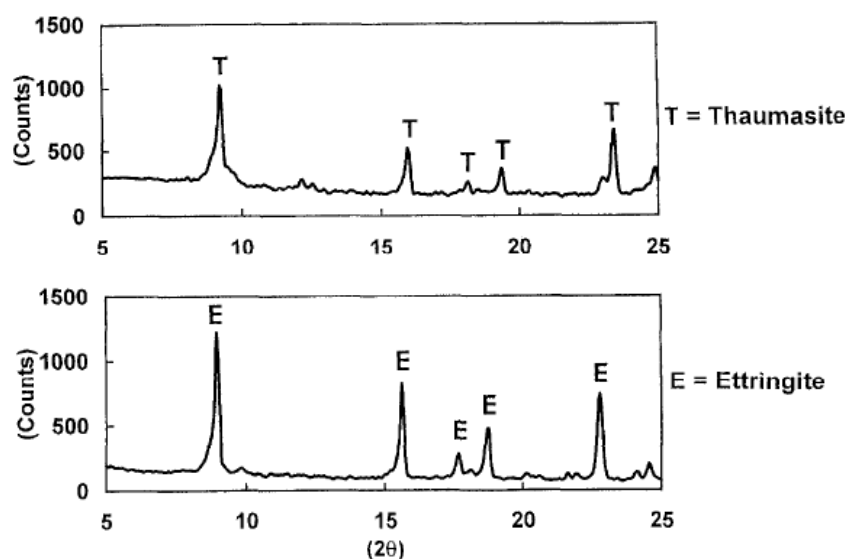


Figure 9 Thaumasite and Ettringite XRD patterns (Collepardi, 1999).

Thermal analysis and infrared spectroscopy also provide the identification of thaumasite with possibility of confusion by Ettringite (Bensted, 1977 apud Skibsted et al., 2003). Raman spectroscopy is possible to be used for this propose (Bensted, 1976 apud Skibsted et al., 2003), as low-vacuum scanning electron microscopy (SEM) which requires several steps of preparation of the samples before the investigation (Yang and Buenfeld, 2000).

### 3.3.3 Historical cases

Gypsum, lime, lime-pozzolan mixtures and hydraulic lime were extensively used in constructions before the advent of Portland cement at the end of the 19<sup>th</sup> century, thus for jointing or rendering mortars as for concrete mixtures of masonry walls of historic buildings. In addition, to repair the damaged masonry walls of historic buildings several times Portland cement is used (Collepari, 1999 p. 147). As a result, many historical buildings present thaumasite formation in cementitious materials.

Calcium hydroxide ( $\text{Ca}(\text{OH})_2$ ), when exposed to air, is transformed into  $\text{CaCO}_3$ , which is present as a hydration product from Portland cement or as the original material in hydraulic lime or lime-pozzolan mixtures, and with this all the ingredients (C-S-H, C-A-H and  $\text{CaCO}_3$ ) are available to produce thaumasite and/or ettringite when exposed to the action of water and gypsum (Collepari, 1999 p. 147).

Over recent years, concrete damage from thaumasite formation has been considered an important aspect, and because of that a group of specialists was formed to research this phenomenon at UK. Moreover, in numerous other countries, the thaumasite formation has been reported, mainly across the cooler regions of the northern hemisphere (Thaumasite Expert Group, 1999).

Veniale et al (2003) developed a study carried out on thaumasite efflorescence at mortars used for the brick wall-framework of a church constructed in 1970 located at Annone Veneto, close to Venice, Italy, showing fissures along the brick–mortar joints and scaly detachments of the bricks' surfaces. The damage provoked by this thaumasite formation consist in heaving, curving and spalling of the wall masonry, analyzing the influence of mortar aggregate composition and environmental conditions on thaumasite formation (Figure 10).

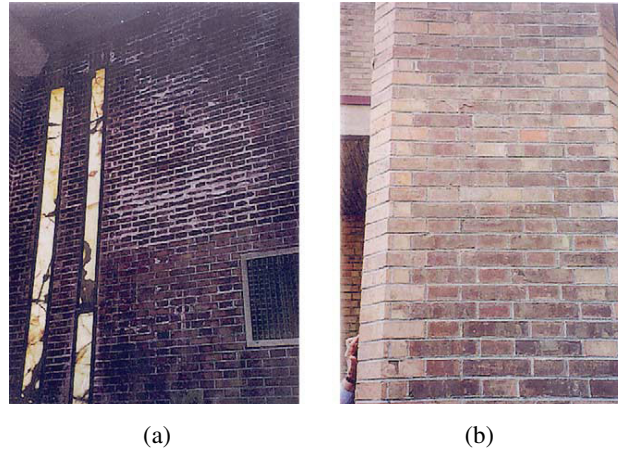


**Figure 10 (a) Thaumasite efflorescence on the internal side of a brick wall exposed to north. (b) External brick wall exposed to south without thaumasite efflorescence (Veniale et al, 2003).**

The sand aggregate of the mortar was composed of carbonates in ranging amounts: calcite 25–40%, dolomite 20–35% and aragonite 5–20%. XRD and SEM were performed and shows that thaumasite is more abundant (20–30%) within mortars of brick walls exposed to the northern side of the perimeter masonry, within mortar pores and between brick/ mortar joints of the masonry walls, especially on the internal side where lack of direct sun radiation, narrow range of temperature changes and dew-condensation conditions actually keep a rather stationary and relatively high room moisture ratio, and low temperature. Noteworthy, the site has cold and humid (foggy) climate during autumn and winter, as conclusions of the authors in this case study.

One important aspect to be considered in historical buildings is the use of repair mortars which can cause the thaumasite formation due to the presence of sulphate salts when the restoration is performed, often present in the masonry itself, particularly when masonry containing sulphate salts is restored by using mortars based on hydraulic binders the risk of failure is evident, according to Corinaldesi et al (2003).

As described by the same authors, when the employment of hydraulic mortars leads to the formation of thaumasite, the plaster deterioration occurs as a progressive removal of mortar washing out by rainwater, because of its alteration into a pulp in wet and cold climates. It can also occur before restoration owing to the employment of pozzolanic mortars, which are hydraulic even if not necessarily cementitious.

The authors analyzed samples of rendering and jointing mortar, removed from two buildings located in the same area in Ancona, Italy, but differently exposed to

various sulphate sources, showed in Figure 11. Deterioration appeared quite similar for both buildings in spite of different exposure to sulphate aggression, which was detected only for rendering and surface jointing mortars through gypsum, ettringite and thaumasite formation. They underline that this evidence makes the environmental sulfation mechanism the most likely one responsible for deterioration attack. Thaumasite and ettringite are evidence of incorrect intervention in this buildings, as their presence in the deterioration products means that mortars were made with hydraulic binders, either original lime–pozzolan or cement used during later interventions, not compatible with sulphate generated by the environmental.

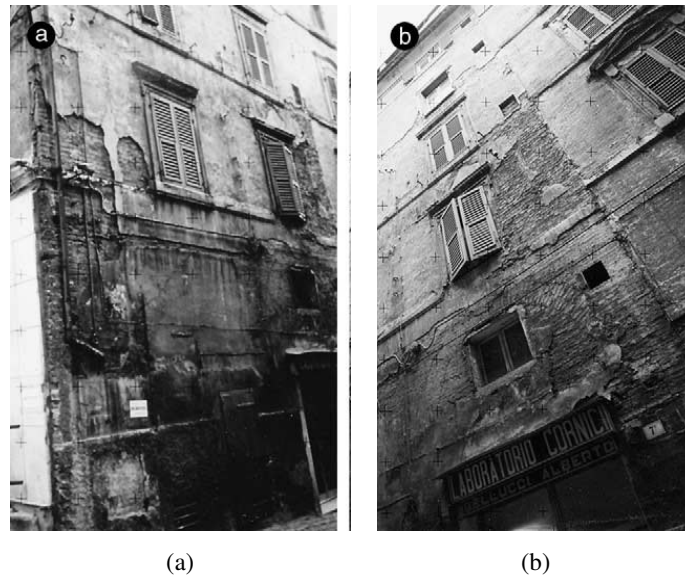


**Figure 11 Deterioration of the rendering mortar caused by ettringite (a) and thaumasite (b) formation in a building located in the historical centre of Ancona (Corinaldesi et al, 2003).**

Van Hees et al (2003) describe that in several case studies in historic buildings in Netherlands, mortar swelling appeared to be the major cause of the damage, and some of this cases have the thaumasite formation as a cause, regarding that it will lead to an expansion of the mortar which can lead to damages to the masonry, the pointing and the bedding mortar and to the masonry units.

The authors describe two cases where thaumasite formation occurs provoking a swelling of the bedding mortar. The first case presented is a historic canal bridge built in 1728 in Amsterdam. The material used was clay brick, externally in good quality with 40 cm and internally a low strength orange–red clay brick, most probably rich in

sulphate. As bedding mortar it was used an hydraulic mortar made by lime–pozzolana binder. The bridge presents damage in the vaults, where push out of the re-pointing made by cement, with presence of chipping of bricks. The bridge is showed in Figure 12.

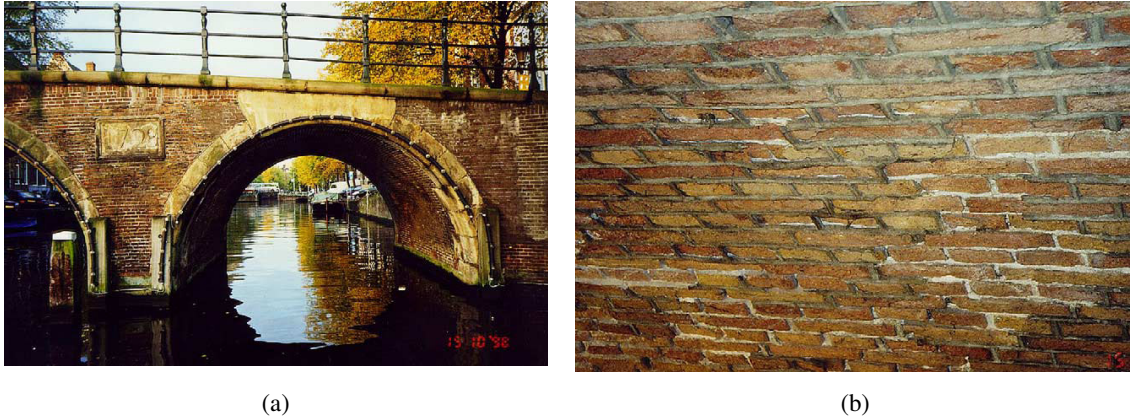


**Figure 12 Bridge in Amsterdam. (a) View. (b) Damage to masonry in vault intrados (van Hees et al, 2003).**

Using polarizing and fluorescent microscopy and SEM/EDAX analysis, the authors found both thaumasite up to a depth of 10 cm from the surface and monochloride. They describe that the formation of thaumasite was due to the use of hydraulic lime as a binder and the ingress of water from the bridge deck and of sulphate originating from the low fired brick used in the internal part of the masonry. Moreover from sulfur oxides from the exhaust gases of the diesel-driven engines of the tourist boats which pass there daily. On the other hand, the formation of monochloride was due to the use of hydraulic lime as a binder and the ingress of chlorides from de-icing salts through the bridge deck before it was replaced by a concrete deck (Van Hees et al, 2003).

The second case presented by van Hees et al (2003) is a church tower built in 1926 in Noordwijk using brick masonry. the external layer was made by a high strength clay brick and the internal with a low strength clay brick rich in sulphate. Just a tooled bedding mortar mainly lime based with some addition of Portland cement were used originally, but later part of the mortar joints have been re-pointed with a cement based mortar. All the wall present visible damage, with vertical and horizontal cracks in the external layer of bricks, vertical cracks through both joints and bricks, horizontal cracks



only through horizontal joints. Moreover severe cracking presenting width up to 17 mm occurs in the upper part of the tower. The damage in the tower is presented in Figure 13.



**Figure 13 Church tower in Noordwijk, with both vertical and horizontal cracks (van Hees et al, 2003).**

Using the same techniques, the authors found thaumasite formation, which has larger volume at bedding mortar and thus the backing brickwork expand. The expansion of the backing masonry caused the cracks in the non-expanding exterior masonry. The diagnosis was that the backing brick was rich in sulphate. Due to ingress of rain water this sulphate migrated into the bedding mortar of the backing masonry, reacting with constituents of the lime-cement to form thaumasite and ettringite (Van Hees et al, 2003).

## 4 MATERIALS AND METHODS

This chapter describes the experimental program, the materials and the analytical techniques used in this study.

### 4.1 Materials

The materials used to prepare the samples are described in the following items.

#### 4.1.1 Cement

Two types of cement were used: Cement I (CEM I 42,5 R) and Cement I - Sulphate Resistant (with low C<sub>3</sub>A content - CEM I 42.5 N/SR). The chemical and mineralogical composition of the two cements and FRX is given in Table 5.

**Table 5 Chemical analysis of the cements.**

Elements	CEM I		CEM I - SR	
	Humid way	FRX	Humid way	FRX
SiO <sub>2</sub>	17.94	18.51	18.08	17.84
Al <sub>2</sub> O <sub>3</sub>	4.30	4.55	3.93	3.87
Fe <sub>2</sub> O <sub>3</sub> (total)	4.01	3.50	4.58	4.84
MnO		0.04		0.03
MgO	2.14	2.46	1.64	2.13
CaO	63.25	57.75	64.42	59.09
Na <sub>2</sub> O		0.67		0.56
SO <sub>3</sub>	2.79	7.69	2.74	7.47
K <sub>2</sub> O		1.05		0.90
TiO <sub>2</sub>		0.16		0.14
P <sub>2</sub> O <sub>5</sub>		0.13		0.10
P.F.	3.5		3.02	
CaO free	0.74		1.24	
R.I.	0.48		0.39	
S.E. (Blaine)	4107.12		4204.62	

The mineralogical characterization of the cements was made using X-Ray Diffraction and Fourier Transform Infra-Red, presented in the Figure 14 and Figure 15.

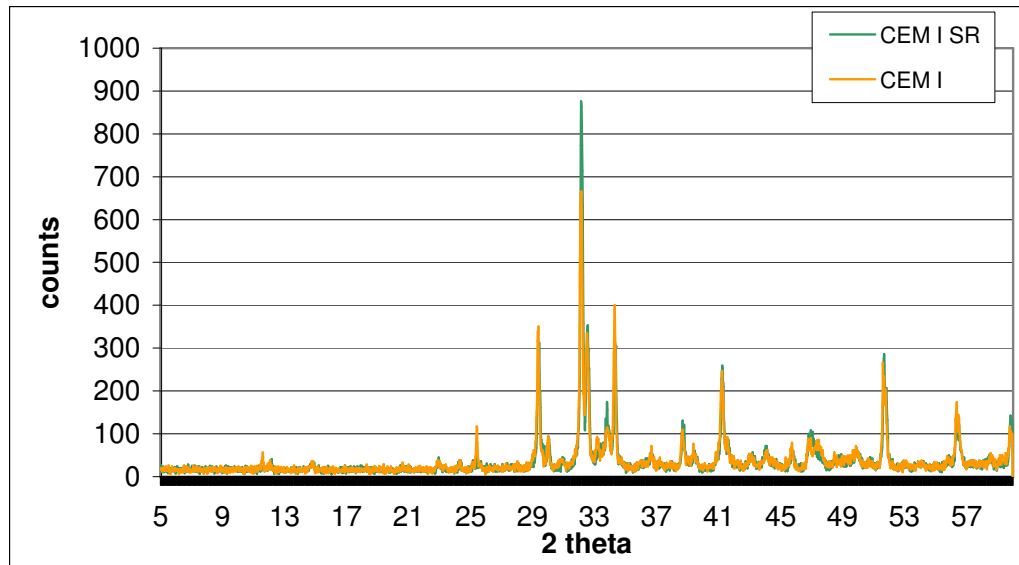


Figure 14 X-Ray Diffraction for the anhydrous cements.

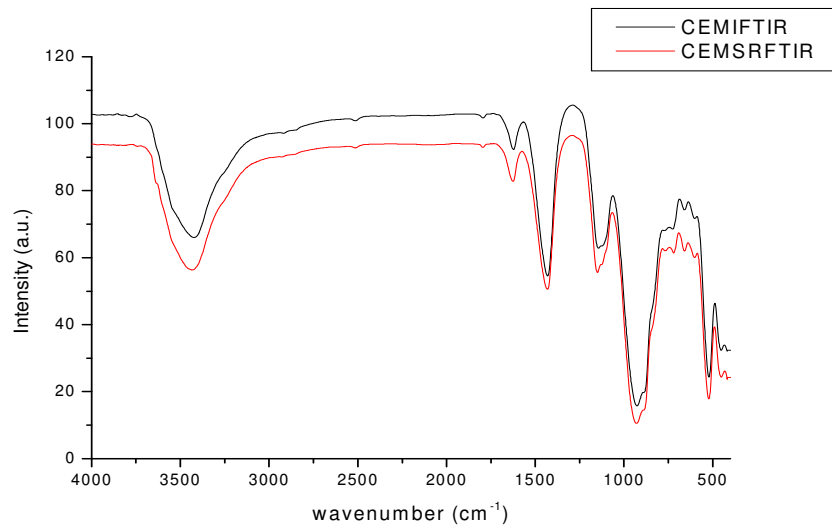


Figure 15 Fourier Transform Infra-Red for the cements.

Low vibration characteristic signal of carbonate groups at 1429, 878 y 717  $\text{cm}^{-1}$  are observed in the FTIR for CEM I. Moreover a large signal with maximum at 948  $\text{cm}^{-1}$  because of the Si-O-Si of  $\text{C}_3\text{S}$  vibrations, also cause of the signal at 517  $\text{cm}^{-1}$ .

The same test for the CEM I – SR shows similar results.

Regarding to the X-Ray Diffraction, the anhydrous compounds of the clinker are identified:  $\text{C}_3\text{S}$ ,  $\beta\text{-C}_2\text{S}$ ,  $\text{C}_4\text{AF}$  and gypsum, and in addition a small amount of  $\text{CaCO}_3$  that justify the value for lose on fire.

The main difference between the cements is the higher amount of  $\text{C}_4\text{AF}$  in the CEM I – SR and the higher intensity of the diffraction lines on the silicate phases of the same cement. On the other hand, the CEM I presents side at  $2\theta$  11.61° regarding to the presence of gypsum.

The particle size of the cements was defined by laser granulometry, presented in Figure 16, and the granulometric distribution is presented at Table 6.

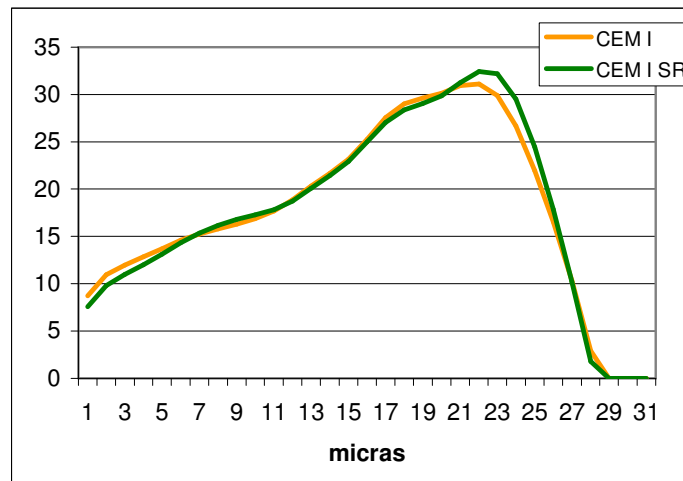


Figure 16 Laser granulometry of the cements.

Table 6 Granulometric distribution of the cements.

	$Q \leq 32 \mu$	$Q \leq 45 \mu$	$Q \leq 90\mu$
CEM I	77.21	87.42	99.60
CEM I SR	75.70	86.59	99.76

### 4.1.2 Silica Fume

In order to determine the influence of silica fume addition in samples a 10% of weight was added. The selected silica fume presented 96.21% of reactive silica. The mineralogical characterization of the silica fume through FTIR and X-Ray diffraction is shown in Figure 17 and Figure 18.



Figure 17 Fourier Transform Infra-Red for the silica fume.

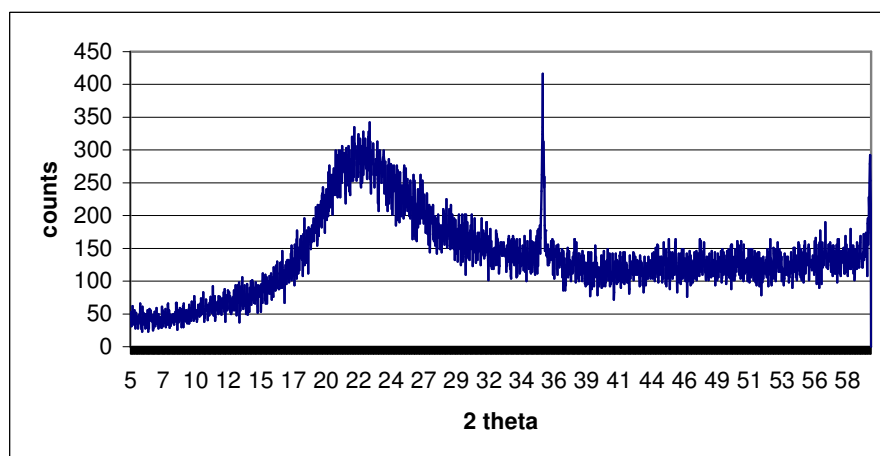


Figure 18 X-Ray Diffraction for the silica fume.

The FTIR spectrum of the silica fume presents three sharp characteristic regions of the silica condensed at signal  $1113 \text{ cm}^{-1}$  where the asymmetric tension vibrations of the Si-O-Si group. In addition, the signal at  $806 \text{ cm}^{-1}$  is regarding to the symmetric

tension vibrations of the same group, and the signal at  $473\text{cm}^{-1}$  is regarding to the deformations of the O-Si-O group.

On the other hand, the X-Ray diffraction for silica fume presents a large side with maximum at  $2\theta=23.8^\circ$  regarding to the presence of an amorphous siliceous composite, and a signal at  $2\theta=35.61^\circ$  regarding to the presence of a siliceous carbonate.

The particle size of the silica fume was defined by laser granulometry, presented in Figure 19, and the granulometric distribution is presented at Table 7.

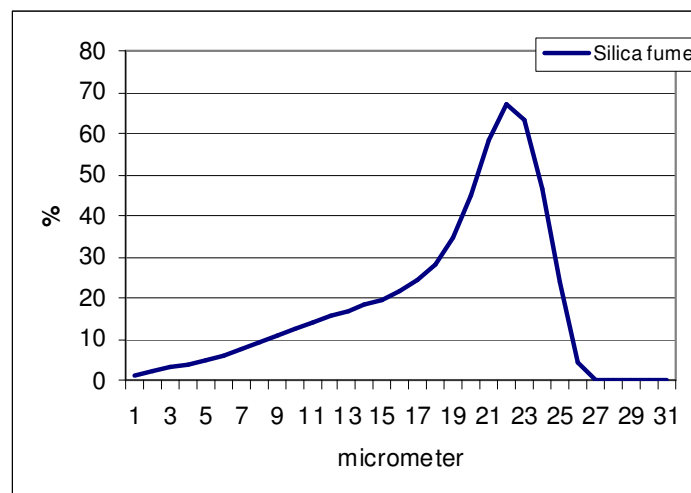


**Figure 19** Laser granulometry of the silica fume.

**Table 7** Granulometric distribution of the silica fume.

	$Q \leq 32 \mu$	$Q \leq 45 \mu$	$Q \leq 90\mu$
Silica Fume	67.68 %	89.00%	100%

## 4.2 Methodology

Pastes specimens were prepared and carbonated in laboratory under carbonation and sulphate conditions. The evolution of the mineralogy of the pastes was monitored through time with the aid of X-Ray Diffraction and Fourier Transform Infra-Red.

In parallel, physical and mechanical properties such as compressive and tensile strength were measured. The data sets were analysed to find interrelationships regarding to understand the effect of CO<sub>2</sub>, temperature and time in the formation of as ettringite and thaumasite.

#### 4.2.1 Experimental set up

The pastes specimens were made with two types of binders, with the following composition:

- CEM I;
- CEM I +10% Silica Fume;
- CEM I-SR;
- CEM I-SR +10% Silica Fume;

The initial and final setting time was determined according to the standard UNE-EN 196-3, and the results are presented in Table 8. For this test, 124 gr of pure cement was used, and for mix with silica fume 133 grams were used, providing a water/cement ratio equal to 0.25 for the cements and 0.27 for the mixtures.

The presence of the silica fume delays the initial setting but accelerate the final setting.

**Table 8 Initial and final setting time.**

	<b>Initial setting</b> (minutes)	<b>Final setting</b> (minutes)
CEM I	135	210
CEM I + 10% Silica Fume	140	195
CEM I SR	150	235
CEM I SR + 10% Silica Fume	173	223

For the resistance tests samples with dimensions 4x4x16 cm were made by mortar with each of the binders, using a cement/sand ratio of 1:3 and a water/cement ratio of 0.5. The samples were cured immersed in water, and tests for compression and flexural strength were made according to the UNE-EN 196-1 at the ages 1, 2, 7 and 28 days. The results are presented in the item 5.1.2.

Specimens of 1x1x6 cm size were produced by mixing the raw materials and using a water/cement ratio of 0.5 (Figure 20). These specimens were cured for 3 months at 21°C and a relative humidity of 95–100% and subsequently subjected to carbonation in chambers at the laboratory, at the following conditions:

- 4% CO<sub>2</sub> concentration and RH=75%:
  - 15 days;
  - 30 days;
- Air carbonation and providing humidity twice a day:
  - 15 days;
  - 30 days;



**Figure 20 Samples.**

The relative humidity for the first samples was assured using a recipient with water saturated with NaCl inside the carbonation chamber to maintain it at 75% (Figure 21). In this case the CO<sub>2</sub> was inserted in the chamber twice a day. In the air carbonation the air was circulated for one hour twice a day by a ventilator.





**Figure 21 Samples at carbonation chambers.**

After this carbonation period, the samples were immersed in a sulphate solution by distilled water with  $\text{CaSO}_4$  in a concentration of 4500 ppm and stored at laboratory temperatures until the immersion time, when they were putted in the refrigerator at constant temperature of  $9^\circ\text{C}$ .

According to this, the ages of the tests are described in the Figure 22.

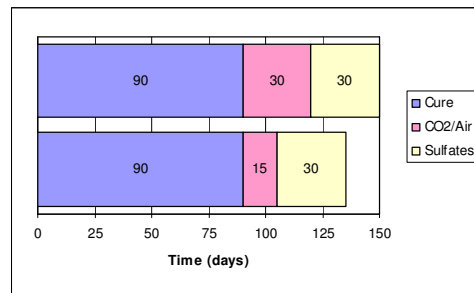


**Figure 22 Ages of the tests.**

### **4.3 Analytical methods**

Paste specimens were grounded (Figure 23) and the hydration process stopped using alcohol and acetone (Figure 24). X-Ray Diffraction and Fourier Transform Infra-Red of the pastes were performed at the following times: end of the cure period; end of

the carbonation process (15 and 30 days) and at 30 days of immersion in sulphate solution.

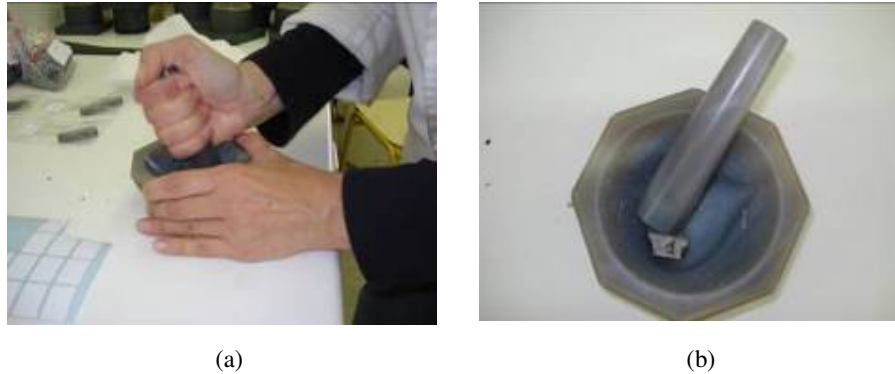


**Figure 23 Samples grinding.**

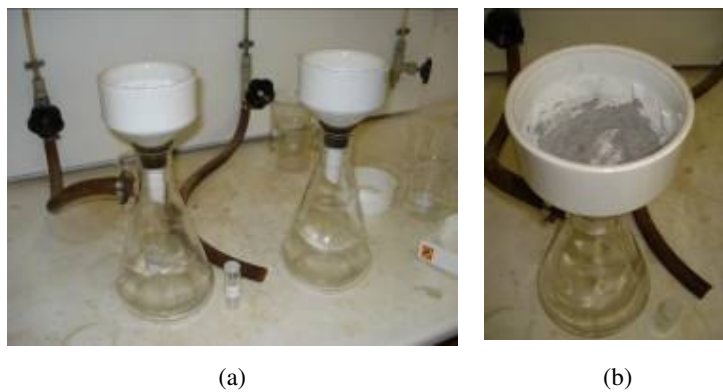


**Figure 24 Stopping the hydration of the Samples.**

#### **4.3.1 X-Ray fluorescence**

The electromagnetic radiation created by X-Ray have high energy and low wave length. For the X-Ray diffraction test a beam of X-rays is applied in a solid material surface and is diffracted in all directions by the associated electrons at each atom or ion that was in its trajectory, producing a diffraction pattern of spots (ICDD, 2008).

To proceed the test is necessary to obtain an adequate crystal of the material, which have to be sufficiently large, pure in composition and regular in structure, without internal imperfections. This crystal is placed in an intense beam of X-rays producing the regular pattern of reflections, and it is gradually rotated provoking the

disappearing of the previous reflections and the appearance of new reflections, recording the data for every angle and reflection. Finally, the data obtained from the test is combined with a library previous data containing complementary chemical information to produce and refine a model of the arrangement of atoms within the crystal (ICDD, 2008).

When single, pure and regular crystals are analyzed, this test determines the mean chemical bond lengths and angles to within a few thousandths of an Ångström and to within a few tenths of a degree, respectively. Moreover the static and dynamic disorder in the atomic positions can be estimated, which is usually less than a few tenths of an Ångström (ICDD, 2008).

This technique is largely used to identify the micro structural characteristics of crystalline materials, particularly to crystalline phases of clinker or cement anhydrous or hydrated, been possible to find and quantify components with less than one percent abundance in a sample (Taylor et al, 2002)

#### **4.3.2 Fourier Transform Infra-Red – FTIR**

The molecules of composites have specific rotation or vibration frequencies corresponding to discrete energy levels. The resonant frequencies of the molecules are determined by the shape of the molecular potential energy surfaces, the masses of the atoms and by the associated vibrancy coupling, characteristics used in Infra-Red spectroscopy.

The strength of the bond among the atoms in the molecule can be related to the resonant frequencies, as the mass of the atoms, allowing the association between the frequency of the vibrations and a particular bond type.

The infrared spectrum of a sample is obtained by passing a beam of infrared light through it, and the examination of the transmitted light reveals how much energy was absorbed at each wavelength. Regarding to measure all wavelengths at once a Fourier transform instrument can be used, IR light is guided through an interferometer and passing the sample, providing a transmittance or absorbance spectrum and showing which IR wavelengths the sample absorbs. Applying a mathematical Fourier transform

on this signal is possible to have the same spectrum from conventional infrared spectroscopy. With the results of FTIR is possible to know details about the molecular structure of the sample.

This technique is actually more used than the conventional because it is cheaper, regarding that the equipment interferometers have an easier fabrication than a monochromator, used in conventional Infra-Red spectrometry. Furthermore, in this technique to measure a single spectrum is faster because all frequencies information are collected simultaneously, allowing multiple samples to be collected and averaged together, that results in a sensitivity improvement.

For the interpretation of the FTIR data for Calcium Aluminate Sulphate Hydrates, the Table 1 gives the wavebands for each composite.

**Table 9 Infrared Spectral Data for the Calcium Aluminate Sulphate Hydrates (Source: Bensted, J. An Infrared Spectral Examination of Calcium Aluminate Hydrates and Calcium Aluminate Sulphate Hydrates encountered in Portland cement Hydration).**

<b>Ettringite Wavebands (cm<sup>-1</sup>)</b>	<b>Interpretation</b>
420 m	$\nu_2$ , SO <sub>4</sub>
550 s	$\nu$ AlO <sub>6</sub>
620 s	$\nu_4$ , SO <sub>4</sub>
855 w	Al-O-H bending
1120 vs	$\nu_3$ , SO <sub>4</sub>
1640 m	
1675 s	$\nu_2$ , H <sub>2</sub> O
3420 vs	$\nu_1$ , and $\nu_3$ , H <sub>2</sub> O
3635 m	$\nu$ OH free

## **5 RESULTS AND ANALYSIS**

### ***5.1 Binder systems before carbonation exposure***

Before the exposition of the samples to carbonation, tests were performed aiming to characterize the it, which results will be described below.

#### **5.1.1 Influence of type of cement**

The X-ray diffraction results for the initial conditions of the four different types of pastes analyzed is described in Figure 25. It shows differences among the hydrated products at the samples, such as the higher content of C-S-H in cement sulphate resistant. Moreover, the portlandite formed is considerably lower in the samples made with silica fume addition. The amount of ettringite formed is similar for all the samples.

There are no important differences between the specimens with cement I and sulphate resistant, and any of the samples present carbonates.

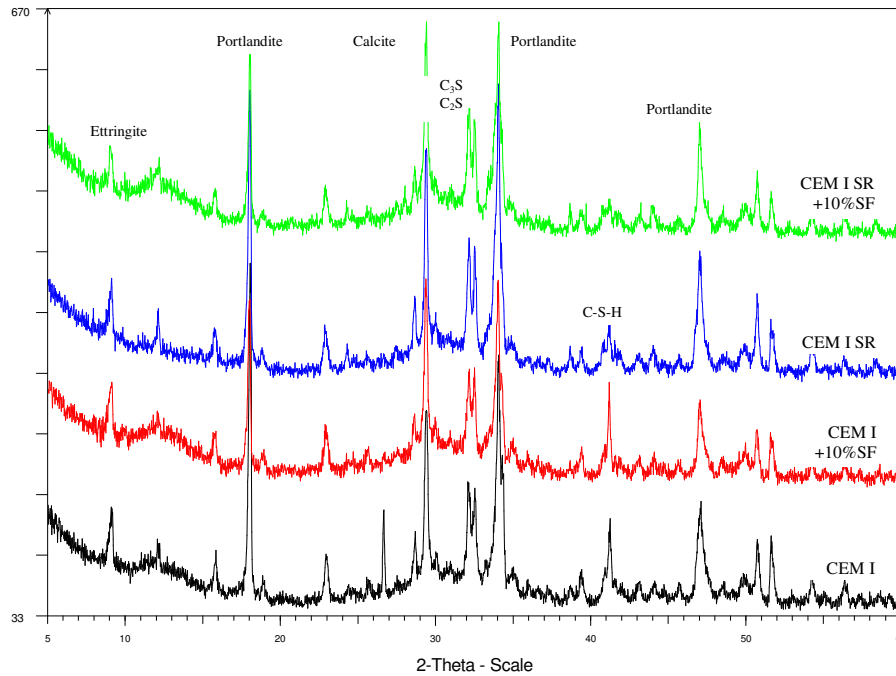


Figure 25 X-Ray diffraction results of Portland cement systems before start the carbonation.

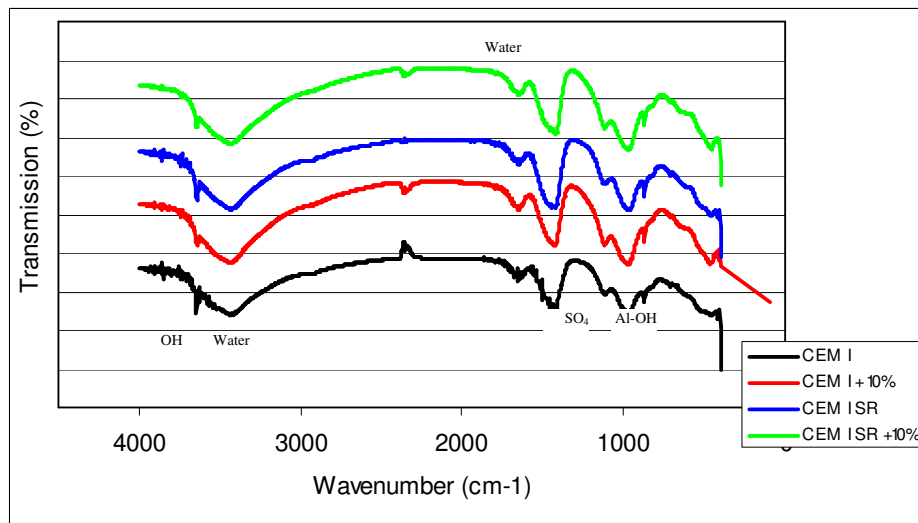


Figure 26 FTIR results of Portland cement systems before start the carbonation.

There are not significant difference among the samples compositions at X-Ray diffraction or FTIR results in this initial stage, that shows the composition are quite similar. It is possible to detect some water, and also the portlandite formed due to the hydration, as the others hydration products.

The Calcium hydroxide is also present, besides the ettringite as an hydration product.

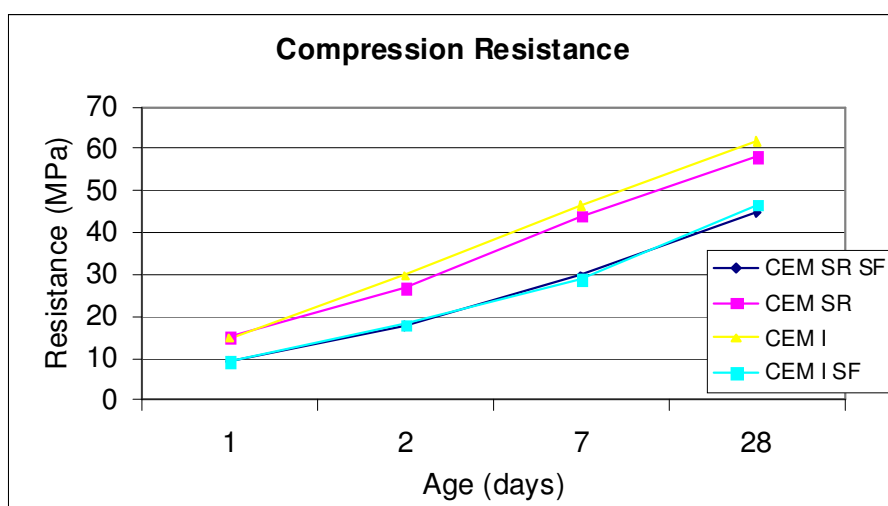
Regarding to the FTIR results, it shows a major absorption bands of ettringite at CEM I and CEM I SR specimens, and this is lower in samples with silica fume addition.

### 5.1.2 Mechanical Tests

As described before, for the resistance tests samples with dimensions 4x4x16 cm were made by mortar with each of the binders. Tests for compression and flexion were made according to the UNE-EN 196-1 at the ages 1, 2, 7, 28 and 200 days. The results are presented in the following tables and figures.

**Table 10 Compression Strength of the mortars.**

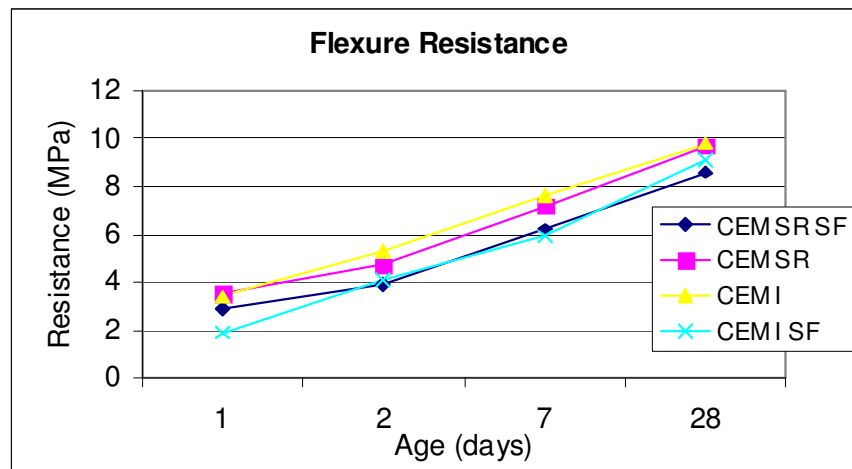
Sample	Compression Resistance (MPa)				
	1 day	2 days	7 days	28 days	200 days
CEM I	14.8±0.2	29.8±0.6	46.5±1.0	61.9±1.1	95.2 ± 5.6
CEM I+ HS	9.2±0.1	18.1±0.7	28.9±1.2	46.9±0.9	99.3 ± 1.8
CEM I SR	15.1 ± 0.5	26.8 ± 0.83	44.0 ± 0.9	58.1±1.9	86.9 ± 4.1
CEM I SR + HS	9.4±0.3	12.8±0.3	29.7±1.0	44.6±1.5	97.9 ± 3.7



**Figure 27 Compression Resistance of the mortars.**

**Table 11 Flexure Resistance of the mortars.**

Sample	Flexure Resistance (Mpa)				
	1 day	2 days	7 days	28 days	200 days
CEM I	3.4±0.1	5.3±0.1	7.6±0.3	9.8±0.3	8.1 ± 0.9
CEM I+ HS	2.9±0.1	4.1±0.3	5.9±0.3	9.1±1	9.1 ± 0.2
CEM I SR	3.5 ±0.4	4.7 ±0.2	7.2 ±0.2	9.7±1.1	7.3 ± 0.1
CEM I SR + HS	2.9±0.2	3.9±0.3	6.2±0.5	8.6±0.6	5.1 ± 0.5

**Figure 28 Flexure Resistance of the mortars.**



## 5.2 Binder systems after carbonation exposure

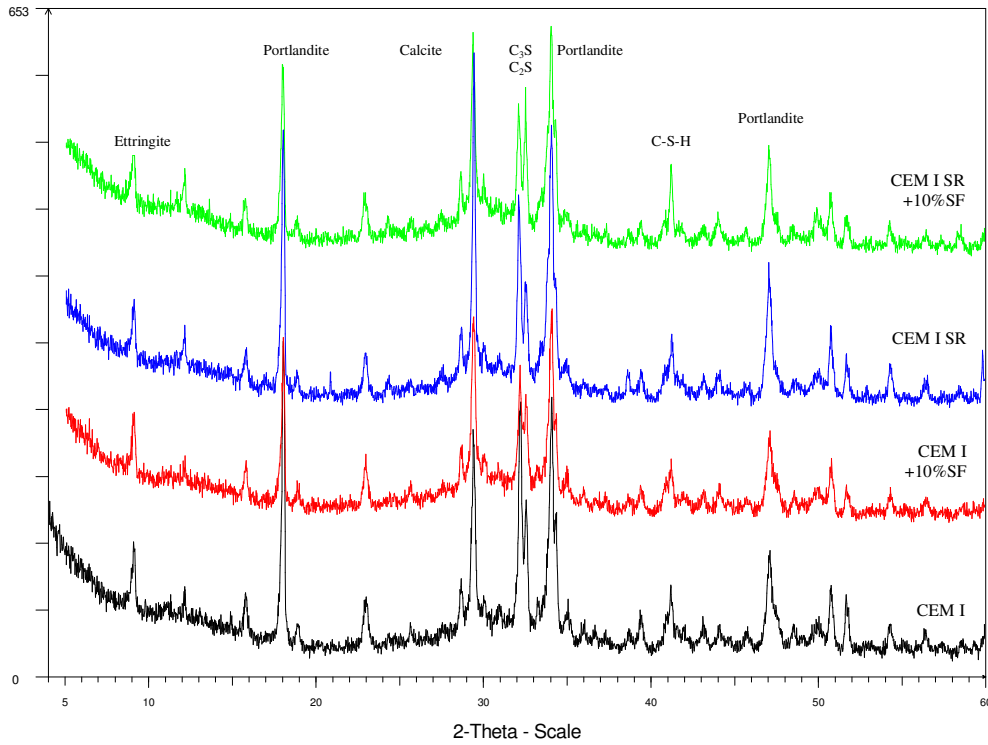


Figure 29 X-Ray diffraction results of Portland cement systems after 15 days of CO<sub>2</sub> exposition.

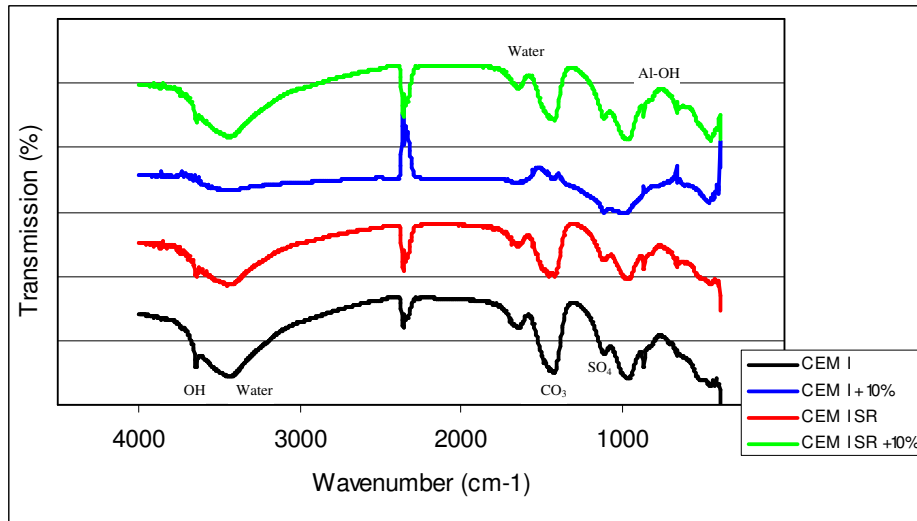


Figure 30 FTIR results of Portland cement systems after 15 days of CO<sub>2</sub> exposition.

It is possible to identify after 15 days of exposure a considerable increasing of the  $C_2S$  and  $C_3S$  content, expected to happen with the progress of the cement hydration. Besides the C-S-H content is increasing for the same reason.

The specimen made by CEM I presents monocarboaluminate formation. In all the samples, the calcite content is increased.

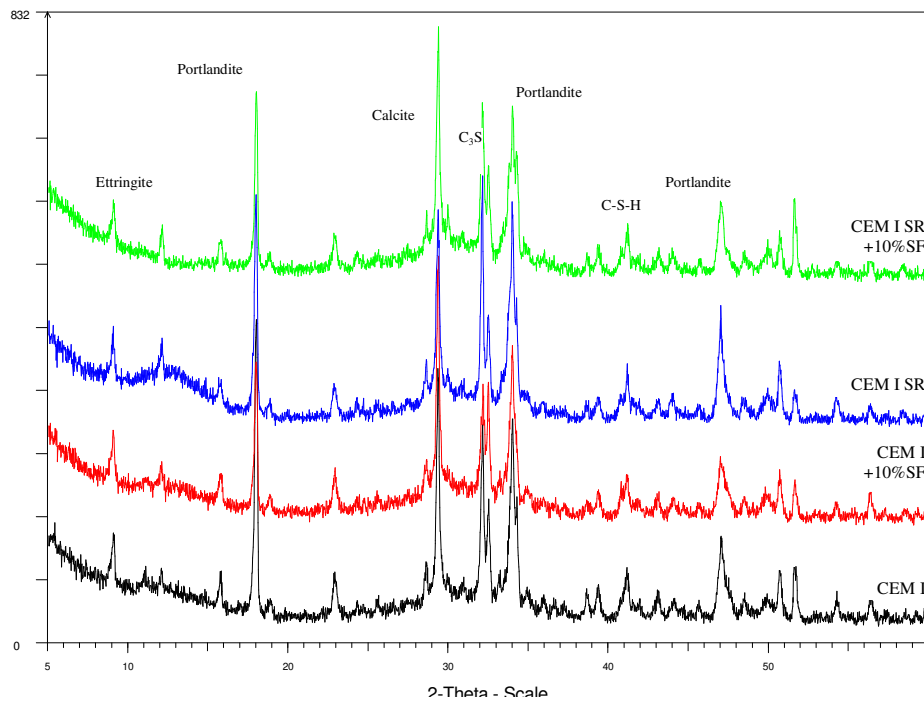


Figure 31 X-Ray diffraction results of Portland cement systems after 30 days of  $CO_2$  exposition.

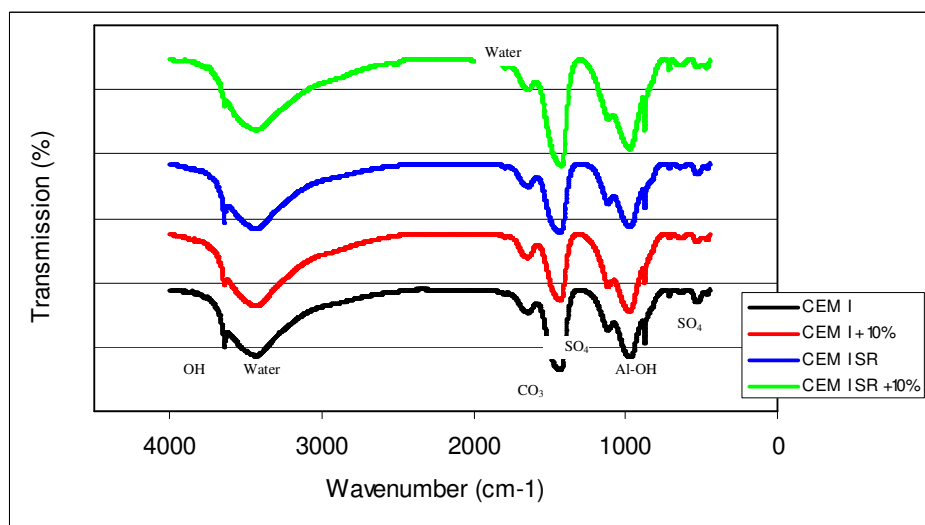
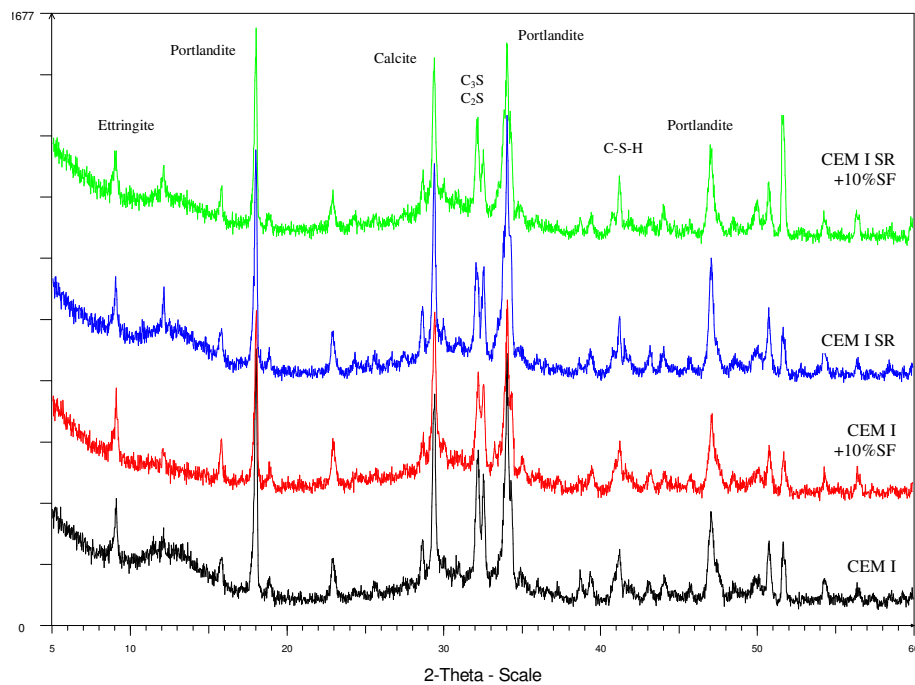


Figure 32 FTIR results of Portland cement systems after 30 days of  $CO_2$  exposition.

In this situation, the specimens made using sulphate resistance cement present a lower quantity of free OH.

Following the same tendency, after 30 days of Carbonic gas exposition the  $C_2S$  and  $C_3S$  content are still growing, expected to happen with the progress of the cement hydration. Besides the C-S-H content is increasing.

The sample CEM I presents a major content of carbonates and monocarboaluminate, but the presence of silica fume or the variation between the different types of cement is not affecting the results.



**Figure 33 X-Ray diffraction results of Portland cement systems after 15 days of air exposition.**

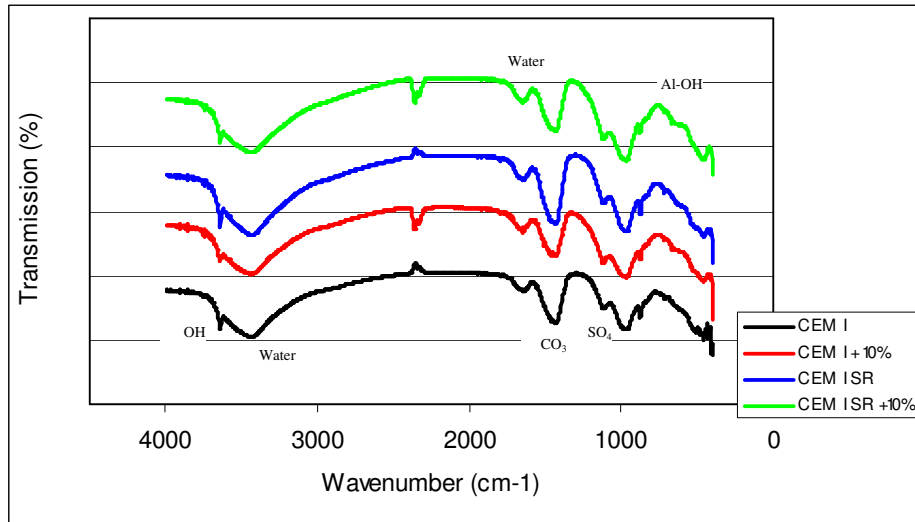


**Figure 34 FTIR results of Portland cement systems after 15 days of air exposition.**

In the same way, in the samples submitted to the carbonation by air exposition is possible to identify an increasing of the  $C_2S$  and  $C_3S$  content, but lower than in the samples submitted to  $CO_2$ . This samples present less carbonation than in samples carbonated with 4%  $CO_2$ .

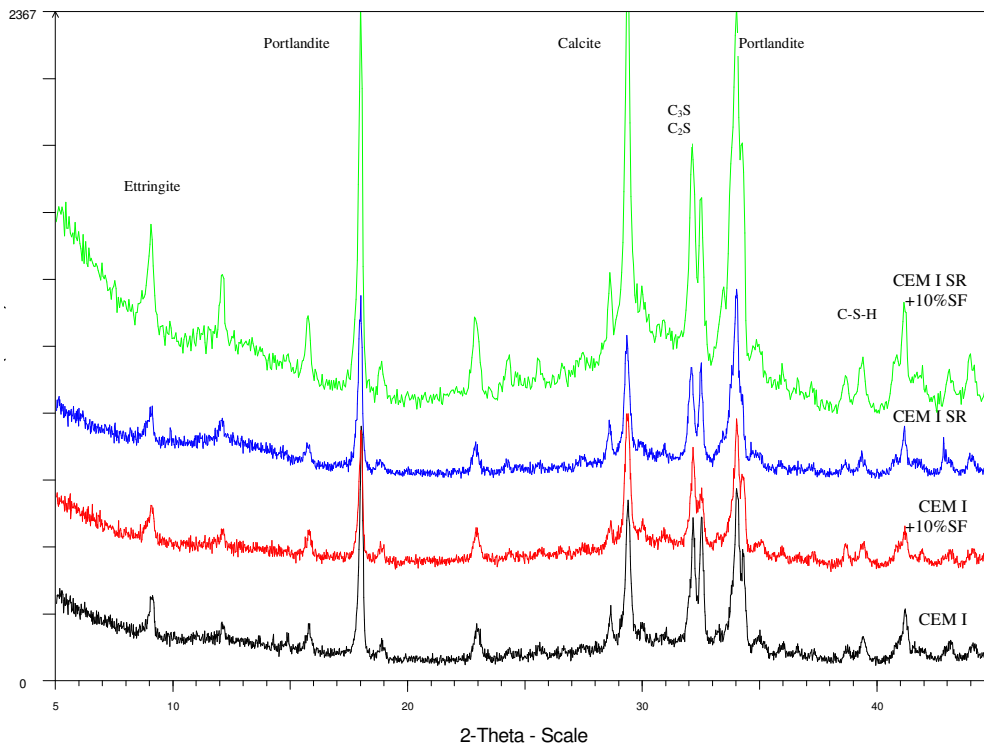


**Figure 35 X-Ray diffraction results of Portland cement systems after 30 days of air exposition.**

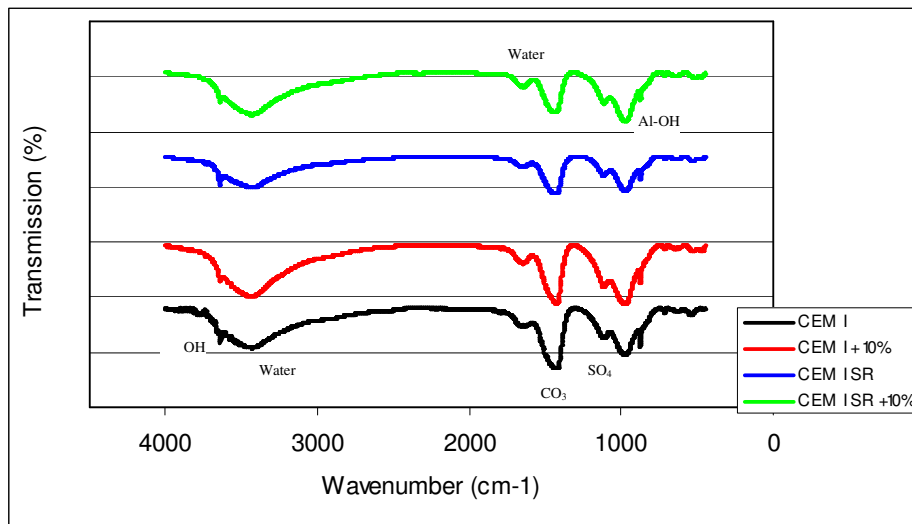


**Figure 36 FTIR results of Portland cement systems after 30 days of air exposition.**

This samples present less carbonation than in samples carbonated with 4% CO<sub>2</sub> and the presence of silica fume or the variation between the different types of cement is not affecting the results.

In all this carbonated samples is possible to identify with X-Ray diffraction the increasing of CaCO<sub>3</sub>, formed as a product of the carbonation reaction and producing water which can be identified in the FTIR graphs.

The presence of monosulphate is also evident due to the hydration process, and the ettringite amount is increasing.

It is clear the development of this carbonation products during the time, comparing the ages of 15 and 30 days of exposition. Besides the amount of carbonation products formed in the samples submitted to carbonation at 4% CO<sub>2</sub> is higher than in samples submitted just to air ventilation.

The FTIR results show a major carbonate absorption bands specially in 30 days samples, as expected.

### 5.2.1 Influence of carbonation system

As already described, the carbonation process shows influence at the products formed in the paste samples, such as  $\text{CaCO}_3$  formed as a product of the reaction between  $\text{CO}_2$  and  $\text{Ca(OH)}$ , in presence of water.

### 5.3 Binder systems after sulphate exposure

After the carbonation of the specimens, with the immersion in sulphates, the X-Ray diffraction and FTIR results are presented below.

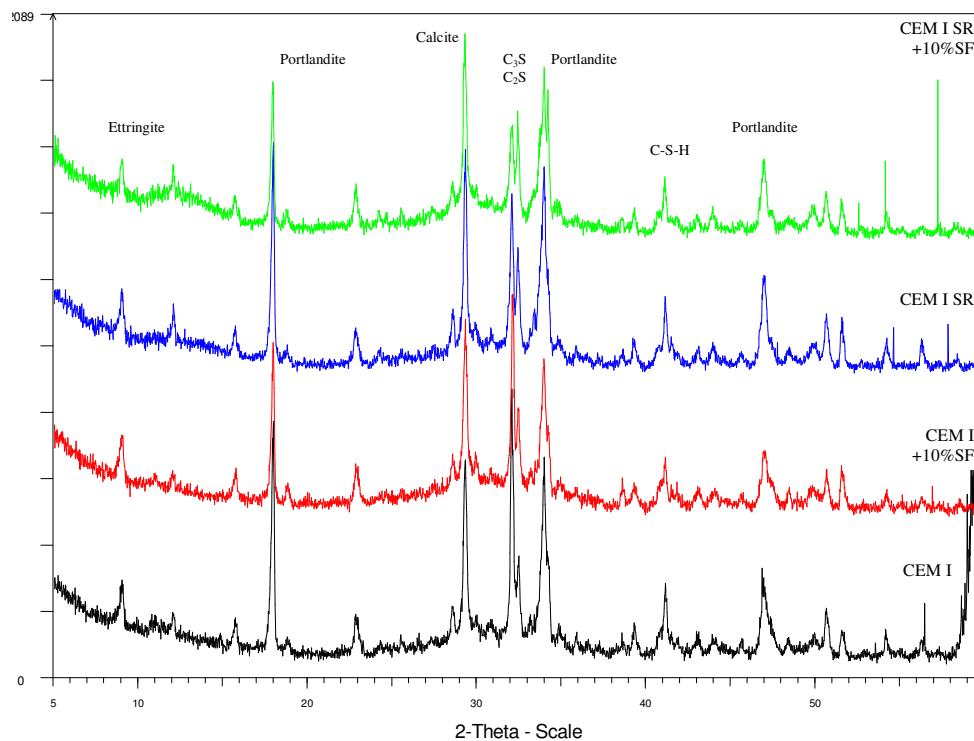


**Figure 37 X-Ray diffraction results of Portland cement systems after 15 days of  $\text{CO}_2$  exposition and 30 days of sulphate exposition.**

In the specimen CEM I the  $\text{C}_3\text{S}$  and  $\text{C}_2\text{S}$  content is considerably higher than the others in this case. The ettringite formation is increasing.

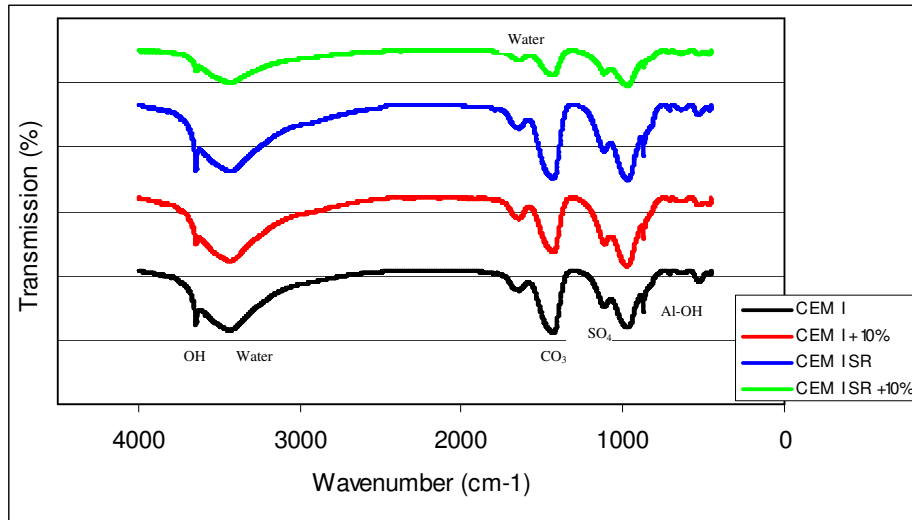


**Figure 38 FTIR results of Portland cement systems after 15 days of CO<sub>2</sub> exposition and 30 days of sulphate exposition.**

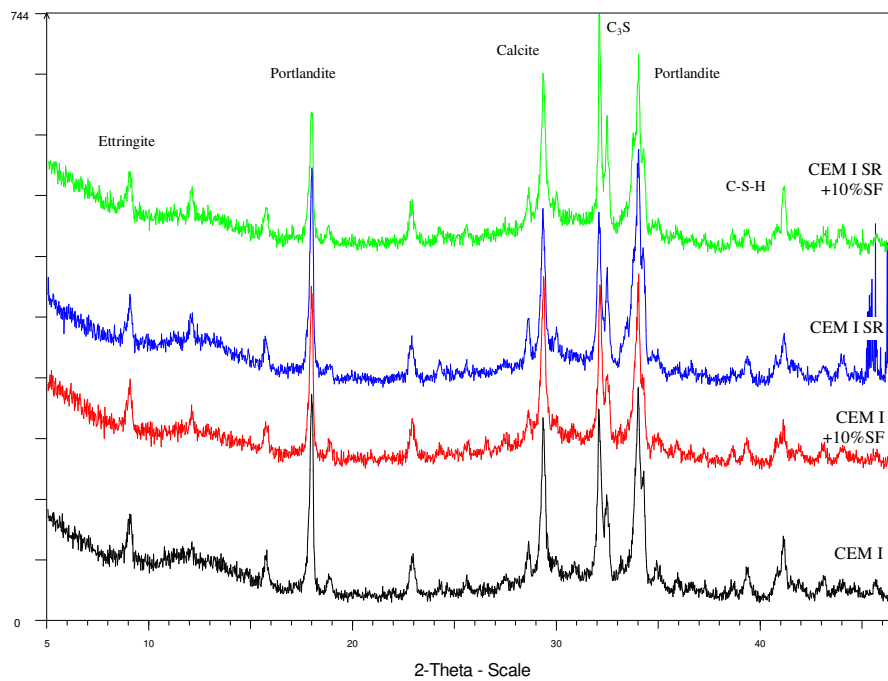


**Figure 39 X-Ray diffraction results of Portland cement systems after 15 days of air exposition and 30 days of sulphate exposition.**

After 30 days of sulphate exposure a considerable increasing of the C<sub>2</sub>S and C<sub>3</sub>S content can be seen, been more accentuated in CEM I SR + 10%. Besides the C-S-H content is increasing, for the same reason. In addition, it is possible to identify that this C-S-H enlargement is more accentuated in the same samples.

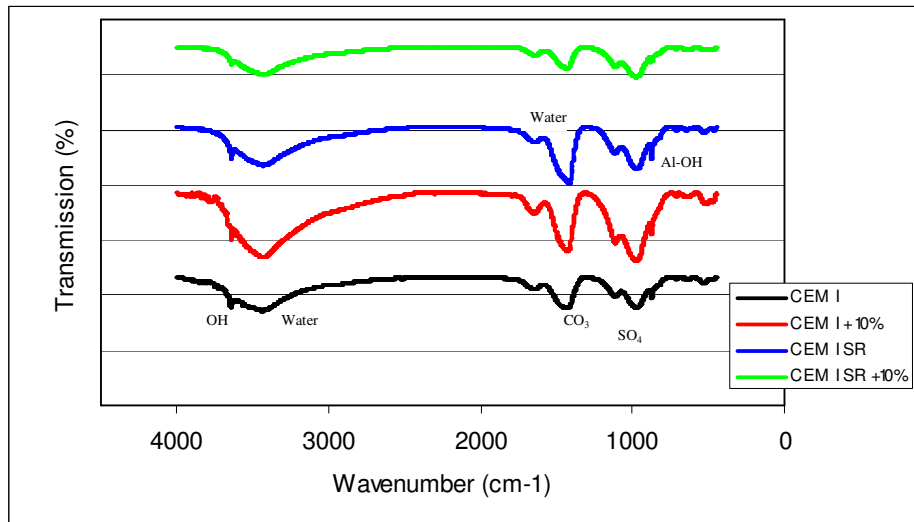


**Figure 40 FTIR results of Portland cement systems after 15 days of air exposition and 30 days of sulphate exposition.**

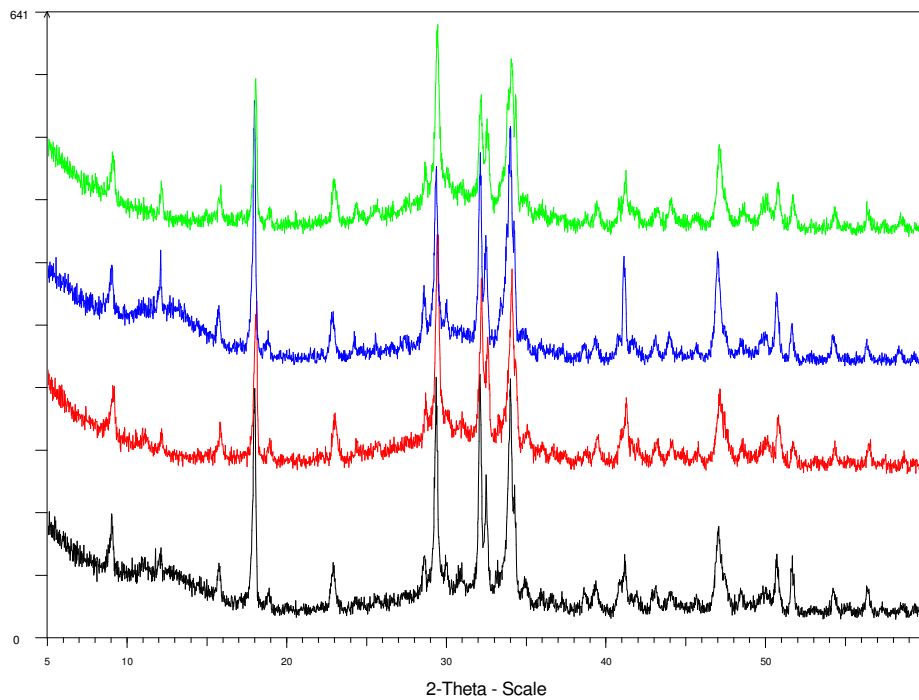


**Figure 41 X-Ray diffraction results of Portland cement systems after 30 days of CO<sub>2</sub> exposition and 30 days of sulphate exposition.**



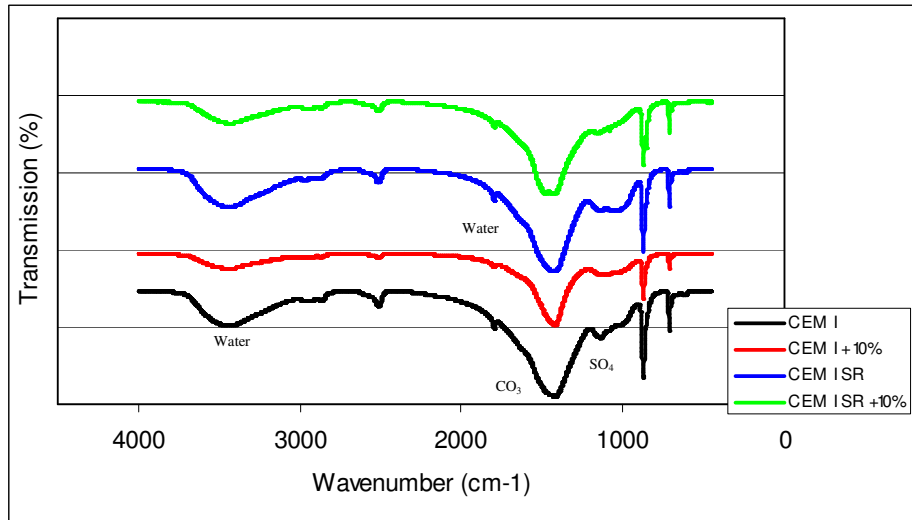


**Figure 42 FTIR results of Portland cement systems after 30 days of CO<sub>2</sub> exposition and 30 days of sulphate exposition.**

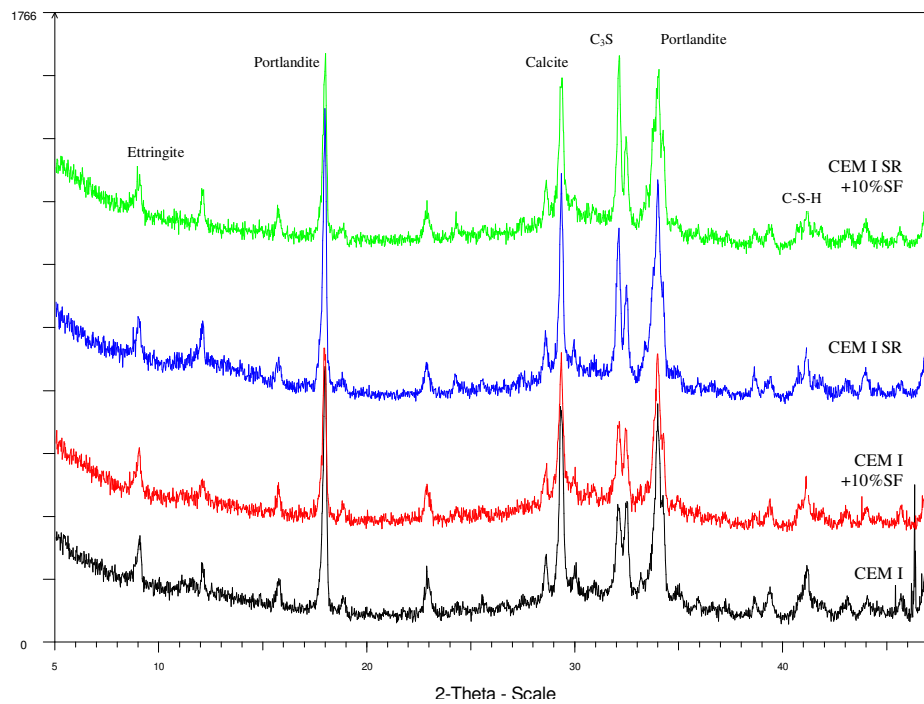


**Figure 43 X-Ray diffraction results of Portland cement systems after 30 days of air exposition and 30 days of sulphate exposition.**

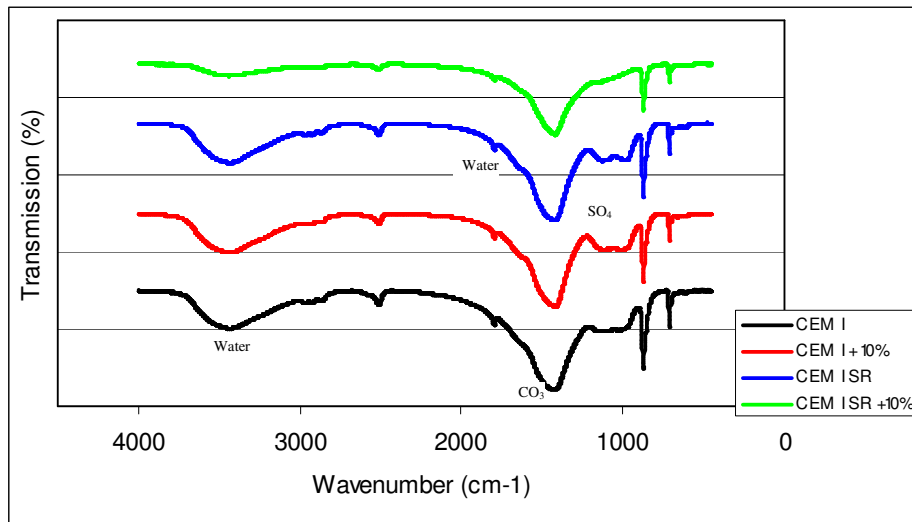


**Figure 44 FTIR results of Portland cement systems after 30 days of air exposition and 30 days of sulphate exposition.**

With the exposure of the samples to sulphate attack, the intensity of carbonate phases is decreasing, as the formation of ettringite is higher. It is also possible to identify some differences in the monosulfate and monocarbonate area in X-Ray diffraction. In these results, the line diffraction of AFm phases is starting to be seen.

Related to the FTIR of the sulphated specimens, it is possible to see an increase of ettringite absorption bands.

At this stage, with the source of sulphates, the monosulphoaluminates react with the sulphates and carbonates and form the ettringite, which increase is evident in all the specimens. Besides, it is possible to identify the gypsum formation due to the reaction of the sulphates with C-S-H, decreasing also the amount of portlandite in the specimens.

It is not possible to identify thaumasite formation due to the early ages, regarding that this phase has a slow velocity in the beginning.

## 6 FINAL CONSIDERATIONS

This dissertation constitutes a State of Art on sulphate attack and thaumasite formation but also a research on this aspect. The State of the Art have shown that the sulphate attack is an important area in which still several research has to be done in order to explain the different unknown mechanisms of the sulphate attack processes.

Regarding to the experimental work developed, this study was focused on sulphate attack and the thaumasite formation in samples submitted to carbonation and external sulphate attack process. It involved experimental and microstructural investigations, of two different cements, the study of silica fume addition, carbonation and sulfate exposure were studied systematically.

The X-Ray diffraction and Fourier Transformer Infrared spectroscopy were techniques used with a good agreement to identify carbonation, sulphate attack and thaumasite formation and apply the results in the deterioration of historical constructions.

### 6.1 *Conclusions*

Finally, the following conclusions can be drawn from the present research:

Sulphate attack is an important degradation process that acts in historical constructions which presents ancient cement as a material, or mortar repair in masonry structures. In this context, thaumasite by sulphate attack is the most serious types of deterioration associated with sulphates.

In this research, the X-ray diffraction and FTIR results allow to identify the composites formed during the cement hydration, carbonation and sulphate attack process. On the other hand, it does not provide very clear information about the thaumasite formation regarding that its similarity with the ettringite. It would be useful the develop a study with complementary techniques helping in the identification of this compound.

During the analysis it was possible to identify differences among of hydrated products in the samples, such as C-S-H, portlandite and ettringite.

In the initial stage, before the carbonation, the samples compositions do not present significant difference by X-Ray diffraction or FTIR.

#### Carbonation effect:

After the carbonation, it is possible to identify an increasing of the  $C_2S$ ,  $C_3S$  and C-S-H content regarding to the progress of the cement hydration. Besides the content is increasing, for the same reason.

The samples submitted to the carbonation by air present a lower content of  $C_2S$  and  $C_3S$  content than the samples carbonated with 4% of  $CO_2$ .

In all this carbonated samples, it is possible to identify with X-Ray diffraction and also with FTIR the increasing of  $CaCO_3$ , formed as a product of the carbonation reaction. The presence of monosulphate and the ettringite amount increase during this process.

The carbonation process provokes the reaction between  $CO_2$ ,  $Ca(OH)_2$  and water, forming  $CaCO_3$ . Comparing the ages of 15 and 30 days of exposition to 4% of  $CO_2$  and air it is clear the development of the carbonation products, and the amount of carbonation products formed in the samples submitted to carbonation at 4%  $CO_2$  is higher than in samples submitted to air.

#### Sulphate effect:

The effect of sulphates over the samples, at these early ages, shows a decrease in carbonates and an increase in ettringite development. Moreover some diffraction lines in the gypsum, monosulphate and monocarbonate area has been detected but in a very initial stage.

In general, it was not observed differences in the obtained results between the type of cement and the presence or not of silica fume in specimens.

During the time available to the development of this research it was not possible to detect the thaumasite formation due to the early ages. The continuity of the tests should present this expected results.

## ***6.2 Suggestions for future researches***

This dissertation is part of a work which is still been developed. Different techniques to analyze the compounds formed will be used to perform its identification. Nevertheless, tests at later ages of sulphates exposition will be performed. It is expected that with these situations, better conditions of thaumasite formation will be observed, been possible to have a more precise understanding of the process.

The thaumasite formation is a slow process due to the fact that the condition formations normally request low temperatures. Regarding on this fact, it is interesting for this study to proceed the analysis at later ages.

As presented before, the thaumasite characterization is difficult to be realized using X-Ray diffraction and FTIR. Besides that, it would be interesting to continue this study using complementary techniques such as magnetic resonance, which provides a better identification of thaumasite formation due to the different coordination of aluminum in this compound with respect to the aluminum coordination in other typical cement phases.

## BIBLIOGRAPHY

BALEN, K. V., et al. **Environmental Deterioration of Ancient and Modern Hydraulic Mortars**. European Commission - Protection and Conservation of European Cultural Heritage. Research Report XX. 216p. 1999.

BENSTED, J. Thaumasite—direct, woodfordite and other possible formation routes. **Cement & Concrete Composites**. 25 (2003) 873–877.

BLANCO-VARELA, M.T. et al. Effect of cement C3A content, temperature and storage medium on thaumasite formation in carbonated mortars. **Cement and Concrete Research** 36 (2006) 707 – 715.

CASSAR, May. **Technological Requirements for solutions in the conservation and Protection of Historic Monuments and Archeological Remains**. European Parliament - Division for Industry, Research, Energy, Environment and STOA (Scientific and Technological Options Assessment). Final Study. Working paper for the STOA Unit. 52p. 2001.

COLLEPARDI, M. A state-of-the-art review on delayed ettringite attack on concrete **Cement and Concrete Composites**, 25 (2003) 401-407.

COLLEPARDI, M. Thaumasite formation and deterioration in historic buildings. **Cement and Concrete Composites** 21 (1999) 147-154.

CORINALDESI, V. et al. Thaumasite: evidence for incorrect intervention in masonry restoration. **Cement & Concrete Composites**. 25 (2003) 1157–1160.

CRAMMOND, N. The occurrence of thaumasite in modern construction – a review. **Cement & Concrete Composites** 24 (2002) 393–402.

European Standards EN 196-1.1994, Methods of Testing Cement. Part 1: Determination of Strength.

European Standards EN 196-3.1994, Methods of testing cement. Part 3: Determination of Setting Time and Soundness.

HOBBS, D.W. Thaumasite sulphate attack in field and laboratory concretes: implications for specifications. **Cement & Concrete Composites**. 25 (2003) 1195–1202.

HOBBS, D.W., TAYLOR, M.G. Nature of the thaumasite sulphate attack mechanism in field concrete. **Cement and Concrete Research**. 30 (2000) 529-533.

ICDD. The International Center of Diffraction Data. Available at: [www.icdd.com](http://www.icdd.com). Access in May, 2008.

JUEL, I. et al. A thermodynamic model for predicting the stability of thaumasite. **Cement & Concrete Composites**. 25 (2003) 867–872.

KIRCHHEIM, A. P. **Cubic and orthorhombic tricalcium aluminate: analysis of in situ hydration and products**. 2008. Tese (Doutorado em Engenharia Civil). Programa de Pós-Graduação em Engenharia Civil, Universidade Federal do Rio Grande do Sul, Porto Alegre, Brasil. [in Portuguese]

KLINOWSKI, J. and MACKAY, A. L. Silicate Structures and Methods for their Analysis. In: **Structures and Performance of Cements**. P. Barnes. Eds. Applied Science Publishers LTD: 1983. p. 1-68. 1<sup>st</sup> Edition.

LOCHER, F. W. **Cement: Principles of Production and Use**. Vbt Verlag Bau U. Technik, 2006

LOZANO, J. A. O. Estudio Experimental sobre la Influencia de la Temperatura Ambiental en la Resistencia del Hormigón Preparado. PhD. Thesis. Politecninc University of Catalunya. Spain. 2005 [in Spanish].

MACPHEE, D., DIAMOND, S. Guest editorial – Thaumasite in Cementitious Materials. **Cement and Concrete Composites** 25 (2003) 805–807.

MEHTA, P. K. Mechanism of sulphate attack on Portland cement concrete – another look. **Cement and Concrete Research** 13 (1983) 401–406.

MEHTA, P. K., MONTEIRO, P. **Concrete: structure, properties e materials**. Prebtuce-Hall. 2<sup>nd</sup> Edition. 548pp. 1993.

OBERHOLSTER, J. H. et al. Durability of Cementitious Systems. In: **Structures and Performance of Cements**. P. Barnes. Eds. Applied Science Publishers LTD: 1983. p. 365-413. 1<sup>st</sup> Edition.

Palomo, A. et al. **Historic Mortars: Characterization and Durability. New Tendencies for Research.**

PÖLLMAN, H., Composition of Cement Phases. In: **Structure and Performance of Cements.** J. Bensted and P. Barnes. Eds. Spon Press: 2002. p. 25-56. 2<sup>nd</sup> Edition.

POPOVICS, S. **Concrete Materials - Properties, Specifications and Testing.** Noyes Publications. New Jersey. 2nd Edition. 673p. 1992.

RAMACHANDRAN, V. S. et al. **Handbook of thermal analysis of construction materials.** Institute for Research in Construction. National Research Council of Canada. Noyes Publications, New York, U.S.A. 2002.

REGOURD, M. Crystal Chemistry of Portland Cement Phases. In: **Structures and Performance of Cements.** P. Barnes. Eds. Applied Science Publishers LTD: 1983. p. 109-138. 1<sup>st</sup> Edition.

SANZ, M. C. **Nuevos Materiales Cementantes Basados en la Activación Alcalina de Cenizas Volantes. Caracterización de Geles N-A-S-H en función del Contenido de Sílice Soluble. Efecto del Na<sub>2</sub>SO<sub>4</sub>.** 2007. Tesis Doctoral. Universidad Autonoma de Madrid. Madrid. Spain. [in Spanish]

SCHMIDT, T. **Sulphate attack and the Role of Internal Carbonate on the Formation of Thaumasite.** 2007. Doctoral Thesis. École Polytechnique Fédérale de Lausanne. Lausanne. Switzerland.

SIBBICK, R. G., CRAMMOND, N. J. **The microscopical characterisation of thaumasite.** Cement & Concrete Composites 25 (2003) 831–837.

SIMS, I. HUNTLEY, S. A. **The thaumasite form of sulphate attack-breaking the rules.** Cement & Concrete Composites 26 (2004) 837–844

SKIBSTED, A. et al. <sup>29</sup>Si cross-polarization magic-angle spinning NMR spectroscopy—  
—an efficient tool for quantification of thaumasite in cement-based materials. **Cement & Concrete Composites** 25 (2003) 823–829.

TAYLOR, H. F. W. **Cement Chemistry.** Academic Press. London. 2nd Edition. 491p. 1990.

TAYLOR, J. C. et al, X-Ray Powder Diffraction Analysis of Cements. In: **Structure and Performance of Cements.** J. Bensted and P. Barnes. Eds. Spon Press: 2002. p. 420-441. 2<sup>nd</sup> Edition.



Thaumasite Expert Group. Report: **The thaumasite form of sulphate attack: risks, diagnosis, remedial works and guidance on new construction**. Department of the Environment, Transport and the Regions, England, 1999.

TORRES, S. M. et al, Thaumasite–ettringite solid solutions in degraded mortars. **Cement and Concrete Research**. 34 (2004) 1297–1305.

VAN HEES, R.P.J. Thaumasite swelling in historic mortars: field observations and laboratory research. **Cement & Concrete Composites**. 25 (2003) 1165–1171.

VENIALE, F. et al. Thaumasite as decay product of cement mortar in brick masonry of a church near Venice. **Cement & Concrete Composites**. 25 (2003) 1123–1129.

YANG R., BUENFELD N. R. Microstructural identification of thaumasite in concrete by backscattered electron imaging at low vacuum. **Cement and Concrete Research**. 2000; 30:775–9.